



LABORATÓRIO NACIONAL
DE ENGENHARIA CIVIL

DEVELOPMENT OF GDams2D 1.0

A MATLAB code for structural analysis of gravity dams using Lagrangian finite elements with 9 nodes

Work carried out under the project P21/LNEC, DAMFA
"Cutting-edge solutions for sustainable assessment
of concrete dam foundations"

Lisbon • September 2019

I&D CONCRETE DAMS

REPORT 321/2019 – DBB/NMMR

Title

DEVELOPMENT OF GDams2D 1.0

A MATLAB code for structural analysis of gravity dams using Lagrangian finite elements with 9 nodes

Authors

CONCRETE DAMS DEPARTMENT

Miguel Ângelo da Silva Rodrigues

Doctoral Research Fellow, Modelling and Rock Mechanics Unit

Sérgio Bruno Martins de Oliveira

Assistant Researcher, Modelling and Rock Mechanics Unit

Copyright © LABORATÓRIO NACIONAL DE ENGENHARIA CIVIL, I. P.

AV DO BRASIL 101 • 1700-066 LISBOA

e-mail: lnec@lnec.pt

www.lnec.pt

Report 321/2019

File no. 0403/112/20755, 0402/112/2075501

DEVELOPMENT OF GDAMS2D 1.0

A MATLAB code for structural analysis of gravity dams using Lagrangian finite elements with 9 nodes

Abstract

In this work we present the version 1.0 of the **GDams2D 1.0** program developed for 2D analysis of gravity dams using the finite element method. This initial version of the program is prepared to analyze the structural behavior of gravity dams for static loads, considering linear-elastic behavior, and using Lagrange finite elements of 4 sides, with 9 nodal points. The **GDams2D 1.0** program, developed in MATLAB, includes a module for automatic generation of meshes with a great level of refinement (generated from coarse meshes of quadrilaterals, with 4 nodal points at the vertices) and is designed for easy adaptation to non-linear analyzes, using stress-transfer modules such as those recently developed for the **DamSlide3D** and **DamDamage3D** programs.

After a brief reference to the fundamentals of solid mechanics and to the simplified hypotheses of plane elasticity, the Fundamentals of the Finite Element Method (FEM) are presented, referring in particular the formulation of the four-node, linear and isoparametric, finite element (FE4nos), with two translation d.o.f per node, and the quadrangular FEs of 9 nodes (FE9nos) used in **GDams2D 1.0**. Based on some examples of application to simple 2D structures whose response is known analytically, the advantages of FEs are emphasized in relation to FE4nos and the verification and operability of **GDams2D 1.0** is made using various discretizations.

Finally, the case of a gravity dam (25 m high) is presented. The dam's structural behavior for the main loads, self-weight and hydrostatic pressure, is simulated with **GDams2D 1.0**. The results obtained are analyzed based on the post-processing module of **GDams2D 1.0**, also developed in MATLAB in the scope of the present work. This module allows several types of representation of the displacement field and stress field.

Keywords: Gravity dams / Linear-elastic behavior / FEM convergence / 2D Lagrangian finite elements / p-refinement and h-refinement / Solid mechanics

DESENVOLVIMENTO DO PROGRAMA GDAMS2D 1.0

Um programa em MATLAB para análise estrutural de barragens gravidade usando elementos finitos de Lagrange com 9 nós

Resumo

Neste trabalho apresenta-se a versão 1.0 do programa **GDams2D 1.0** desenvolvido para análise plana de barragens gravidade utilizando o método dos elementos finitos. Esta versão inicial do programa está preparada para efetuar a análise do comportamento estrutural de barragens gravidade em regime elástico-linear sob ações estáticas, usando elementos finitos de Lagrange, de 4 lados, com 9 pontos nodais. O programa **GDams2D 1.0**, desenvolvido em MATLAB, inclui um módulo para geração automática de malhas com grande nível de refinamento (geradas a partir de malhas largas de quadriláteros, com 4 pontos nodais, nos vértices) e está estruturado para uma fácil adaptação a análises não lineares recorrendo a módulos de “*stress-transfer*” como os recentemente desenvolvidos para os programas **DamSlide3D** e **DamDamage3D**.

Após uma breve referência aos fundamentos da mecânica dos sólidos e às hipóteses simplificativas adotadas em elasticidade plana, apresentam-se os fundamentos do Método dos Elementos Finitos (MEF), referindo em particular a formulação dos EF planos quadrangulares (linear e isoparamétrico) de 4 nós (EF4nos), com duas translações por nó, e dos EF quadrangulares de Lagrange de 9 nós (EF9nos) utilizados no **GDams2D 1.0**. Com base em alguns exemplos de aplicação a estruturas planas simples cuja resposta é conhecida analiticamente, salientam-se as vantagens dos EF9nos relativamente aos EF4nos e efetua-se a verificação e operacionalidade do **GDams2D 1.0** recorrendo a diversas discretizações.

Por fim, apresenta-se como exemplo de aplicação o caso de uma barragem gravidade (25 m de altura) cujo comportamento estrutural para as ações do peso próprio e da pressão hidrostática é simulado com o **GDams2D 1.0**. Os resultados obtidos são analisados com base no módulo de pós-processamento do **GDams2D 1.0**, também desenvolvido em MATLAB no âmbito do presente trabalho, o qual permite diversos tipos de representação do campo de deslocamentos e do campo de tensões.

Palavras-chave: Barragens de gravidade / Comportamento elástico-linear / Convergência do MEF / Elementos finitos 2D Lagrangianos de 9 nós / Refinamento “p” e “h” / Mecânica dos sólidos

Table of contents

1	Introduction.....	1
2	Computational analysis of structures. Fundamental Equations for Plane elasticity	3
	2.1 Computational analysis of structures	3
	2.2 The strain-displacement relation.....	3
	2.3 The stress-strain relations.....	4
	2.4 Equilibrium equation. The relation between stress spatial derivatives and body forces	5
	2.5 Navier's equation	7
	2.6 Weak formulation	8
3	Finite Element Method	9
	3.1 Introductory considerations	9
	3.2 Finite element with 4 nodal points for plane structures	12
	3.3 2D finite element with 9 nodal points	13
4	The Program GDams2D 1.0	15
5	Test Structures	17
	5.1 Introductory considerations	17
	5.2 2D structure.....	17
	5.3 Fixed-fixed supported beam	20
	5.3.1 Analysis of the stress patterns computed in each element	26
6	Gravity Dam. Case Study.....	30
	6.1 Dam presentation.....	30
	6.2 Dam structural behavior modelling	31
7	Conclusions.....	39
	Bibliographic References.....	41

List of figures

Figure 2.1 – Computational analysis of structures using FEM (adapted from Oliveira, S., 2016)	3
Figure 2.2 – Normal strain components (a.) and shear strain components (b.), adapted from (Oliveira, S.; 2016)	4
Figure 2.3 – Constitutive equations. 3D and 2D cases. Plane strain and plane stress (adapted from Oliveira, S., 2016)	6
Figure 2.4 – Body forces, normal and shear stresses acting on a differential element (adapted from DES-UA, 2008)	7
Figure 2.5 – Main equations of Solid Mechanics (adapted from Oliveira, S., 2016)	7
Figure 3.1 – Structural analysis using FEM. Introduction of FEM's fundamental approximation in the integral form of Navier's equation	11
Figure 3.2 – Plain, 4 nodes, isoparametric finite element. The Gaussian interpolation points locations are presented with the red color cross	12
Figure 3.3 – Interpolation functions of the 4 nodal points element.....	13
Figure 3.4 – Isoparametric finite element with 9 nodes (master). The Gauss interpolation points are represented with red color crosses	13
Figure 3.5 – Interpolation functions of the quadrilateral finite element with 9 nodal points	14
Figure 4.1 – MATLAB programming script scheme for the FEM elementar stiffness matrix calculus and subsequent assembly on the global stiffness matrix, considering a 4 nodal points 2D element	16
Figure 5.1 – Test example using a FE mesh with linear elements of 4 nodes (Plane elasticity)	18
Figure 5.2 – Test example. Results from the program GDams2D1.0 (Plane elasticity)	19
Figure 5.3 – Test example using a mesh with linear 4 node elements. Fixed-fixed beam: 22 elements discretization	22
Figure 5.4 – Test example using a mesh with linear 4 node elements. Fixed-fixed beam. 5632 elements discretization	23
Figure 5.5 – Use of Lagrangian 2DFE of 9 nodes (GDams2D1.0). Fixed-fixed beam under SW load: coarse mesh with 22 elements. Displacements and principal stresses.....	24
Figure 5.6 – Use of Lagrangian 2DFE of 9 nodes (GDams2D1.0). Fixed-fixed beam under SW load: fine mesh with 5632 elements (automatically generated with GDams2D1.0 from a coarse mesh). Displacements and principal stresses	25
Figure 5.7 – Mid-span displacement on a fixed-fixed beam under SW load for different mesh refinements	26
Figure 5.8 – Cantilever beam with four serendipity elements with 8 nodes. Stress sampling using 4 Gauss points (2x2) and extrapolation to nodes (Zienkiewicz, O. C. et al., 2005, p. 466) using the shape functions.....	27
Figure 5.9 – Use of linear 2DFE with 4 nodes. Stress analysis: numerical results for σ_{11} and σ_{12} fields considering an increasing h-refinement in a fixed-fixed beam under the SW load.....	28
Figure 5.10 – Use of Lagrangian 2DFE of 9 nodes. Stress analysis (GDams2D1.0): numerical results for σ_{11} and σ_{12} fields considering an increasing h-refinement in a fixed-fixed beam under the SW load.....	29
Figure 6.1 – Gravity dam. On the top left, downstream view (photo). On the top right, the cross section view (Pereira, R.; 2011). On the middle, the site plan. On the bottom, the downstream elevation view (CNPGB, 1992)	30
Figure 6.2 – Dam discretization. Input mesh (FE with 4 nodal points) used for automatic generation of the final mesh with Lagrangian FE of 9 nodes	32
Figure 6.3 – Dam discretization using Lagrangian FE with 9 nodal points (automatically generated with GDams2D1.0)	33

Figure 6.4 – Dam response under self-weight. Displacements and principal stresses (GDams2D1.0)	34
Figure 6.5 – Dam response under hydrostatic pressure. Displacements and principal stresses (GDams2D1.0)	35
Figure 6.6 – Dam response under self-weight and hydrostatic pressure. Displacements and principal stresses (GDams2D1.0)	36
Figure 6.7 – DamSafe1.0. Program for observation data analysis, using effects separation models. Program's main menu, output window for the studied dam. Zoom on the hydrostatic effect graph.....	38

1 | Introduction

“Culture, knowledge and science have worked together, side by side, in many civilizations, old and new, to develop one of the most important and necessary resources available to man: water” (Serafim, J. L.; Clough, R. W., 1990)

Laginha Serafim and Ray Clough, in the introduction of their book on arch dams (Serafim, J. L.; Clough, R. W., 1990), began by emphasizing that for all civilizations, new and old, the control of water resources has always been recognized as a fundamental issue, hence the great importance of dams for modern society.

Nowadays, due to the improvement on numerical methods for solving solid mechanics problems and due to the advances on digital technology, it has been generalized the use of computational models for dam safety control, namely for the simulation of the main aspects of dams behavior using the Finite Element Method (FEM).

The FEM, which was founded with the publication of a set of scientific papers in the 1940s, was firstly developed as a numerical technique for finding approximate solutions to boundary value problems for partial differential equations. This numerical method is based on a problem domain's subdivision into simpler parts, called finite elements (Clough 1960), and on the calculus of variations to minimize an associated error function. The scientific pillars of the finite element method were a direct result of the need to solve complex elasticity and structural analysis problems in civil and aeronautical engineering. The first developments can be traced back to the works of A. Hrennikoff and R. Courant [Hrennikoff, 1941; Courant, 1943]. Although these pioneers used different perspectives in their finite element approaches, they each identified the one common and essential characteristic: mesh discretization of a continuous domain into a set of discrete sub-domains, usually called elements. Since the 1940s, the FEM was continuously developed by several mathematicians and engineers (Argyris 1954; Turner et. al 1956; Clough 1960;1965;1979 ; Clough & Wilson, 1962; Zienkiewicz & Cheung 1967; Oliveira 1968; Zienkiewicz 1971; Strang & Fix 1973; Pedro 1977) and nowadays is the numerical tool most used for computational modeling of physical systems in many engineering disciplines including electromagnetism, heat transfer, fluid dynamics, and, of course, dam behavior, under static and dynamic loads. In what concerns the computational implementation of FEM it should be referred that, in 1965, NASA issued a request for a proposal for the development of the first program for structural analysis using the FEM technology. The result was the program NASTRAN (NASA STRuctural ANalysis), developed by Computer Sciences Corporation (CSC), in 1968. In what concerns the Portuguese contribution for FEM, it is important to highlight the work of Arantes e Oliveira that gave a significant contribution on the mathematical basis of the FEM theory (Oliveira 1968) and the contribution of Oliveira Pedro, that, working alongside with Zienkiewicz, brought the knowledge of this numerical method to Portugal and was the first to apply the FEM to dam structures (Pedro, 1977), starting a long lasting tradition in Laboratório Nacional de Engenharia Civil (LNEC).

In this report we present a FE program, **GDams2D1.0**, developed for 2D analysis of gravity dams using the finite element method. This initial version of the program is prepared to analyze the structural behavior of gravity dams for static loads, considering linear-elastic behavior, and using Lagrange finite elements of 4 sides, with 9 nodal points. The **GDams2D1.0** program, developed in MATLAB, includes a module for automatic generation of meshes with a high level of refinement (generated from coarse meshes of quadrilaterals, with 4 nodal points at the vertices) and is designed for easy adaptation to non-linear analysis, using stress-transfer modules such as those recently developed for the **DamSlide3D** and **DamDamage3D** programs.

After a brief reference to the fundamentals of solid mechanics and to the simplified hypotheses of plane elasticity, the Fundamentals of the Finite Element Method (FEM) are presented, referring in particular the formulation of the four-node, linear and isoparametric, finite element (FE4nos), with two translation d.o.f per node, and the quadrangular FEs of 9 nodes (FE9nos) used in **GDams2D1.0**. Based on some examples of application to simple 2D structures whose response is known analytically, the advantages of FEs are emphasized in relation to FE4nos and the verification and operability of **GDams2D1.0** is made using various discretizations.

Finally, the case of a gravity dam (25 m high) is presented. The dam's structural behavior for the main loads, self-weight and hydrostatic pressure, is simulated with **GDams2D1.0**. The results obtained are analyzed based on the post-processing module of **GDams2D1.0**, also developed in MATLAB in the scope of the present work. This module allows several types of representation of the displacement field and stress field.

2 | Computational analysis of structures. Fundamental Equations for Plane elasticity

2.1 Computational analysis of structures

The Finite Element Method (FEM) is the most used method in computational analysis of structures (Figure 2.1). The main goal is to compute the displacement, strain and stress fields due to external loads.

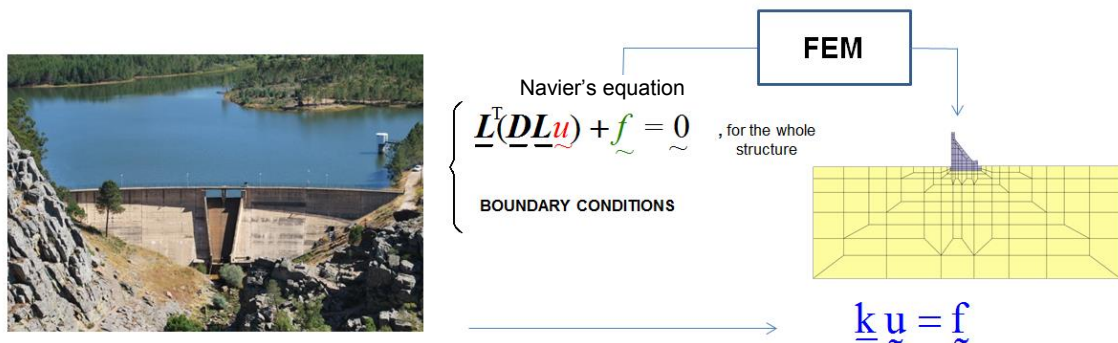


Figure 2.1 – Computational analysis of structures using FEM (adapted from Oliveira, S., 2016)

To obtain the solution for the structural analysis problem it is necessary to know the structure geometry and the physical laws that govern its behavior, namely, how forces, stresses, deformations and displacements relate to each other. Those relationships can be expressed mathematically as a Boundary Value Problem based on the Navier's differential equation $\underline{L}^T(\underline{DL}\underline{u}) + \underline{f} = \underline{0}$ (see Figure 2.1).

In this work is assumed a linear elastic behavior for the materials and the hypothesis of small strains.

2.2 The strain-displacement relation

The normal strain is the measure of how the displacement changes through space, which can be seen as a displacement gradient. Physically, a normal strain component is the unit change in length of a line element (fiber). **Error! Reference source not found.** illustrates, for 2D case, the concept of normal strain components and shear strain components (for small deformations we also have small angular variations so it can be assumed $\alpha = \tan(\alpha)$ and $\beta = \tan(\beta)$, and we can write $\alpha = \hat{\partial}u_1 / \hat{\partial}x_2$, and $\beta = \hat{\partial}u_2 / \hat{\partial}x_1$) (DES-UA; 2008).

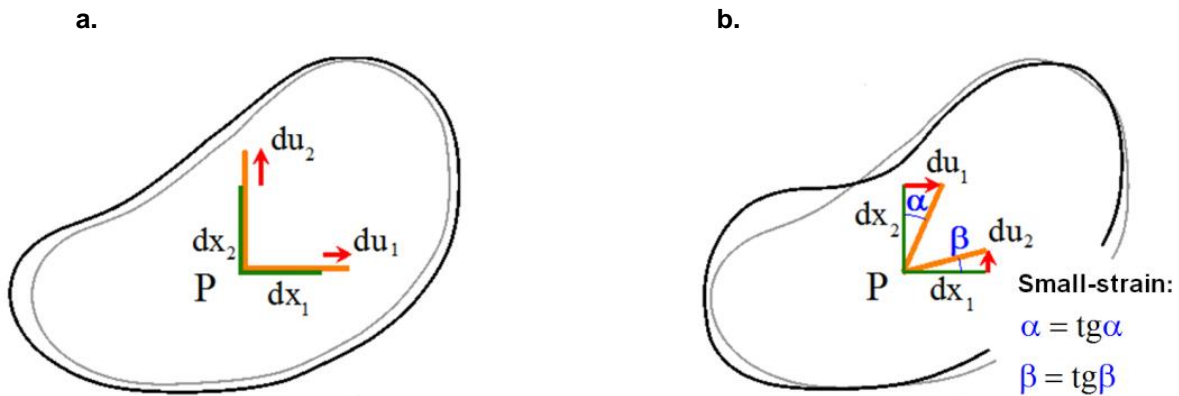


Figure 2.2 – Normal strain components (a.) and shear strain components (b.), adapted from (Oliveira, S.; 2016)

Figure 2.2a. represents schematically the concept of normal strain components at a point P, only with fiber length variation, where $\epsilon_{11} = \frac{\partial u_1}{\partial x_1}$ and $\epsilon_{22} = \frac{\partial u_2}{\partial x_2}$.

In Figure 2.2b. is represented schematically the concept of shear strain components at P, that is related with the angle variation of perpendicular material lines, being $\epsilon_{12} = \epsilon_{21} = \frac{1}{2}(\alpha + \beta) = \frac{1}{2}\left(\frac{\partial u_1}{\partial x_2} + \frac{\partial u_2}{\partial x_1}\right)$.

The strain displacement relation, for the 2D case, is given by the following expression, where \underline{L} is a linear differential operator (Zienkiewicz, O. C. et al., 2005)

$$\left\{ \begin{array}{l} \epsilon_{11} = \frac{\partial u_1}{\partial x_1} \\ \epsilon_{22} = \frac{\partial u_2}{\partial x_2} \\ \epsilon_{12} = \frac{1}{2}\left(\frac{\partial u_1}{\partial x_2} + \frac{\partial u_2}{\partial x_1}\right) \end{array} \right. \Rightarrow \left\{ \begin{array}{l} \epsilon_{11} \\ \epsilon_{22} \\ 2\epsilon_{12} \end{array} \right\} = \begin{bmatrix} \frac{\partial}{\partial x_1} & 0 \\ 0 & \frac{\partial}{\partial x_2} \\ \frac{\partial}{\partial x_2} & \frac{\partial}{\partial x_1} \end{bmatrix} \left\{ \begin{array}{l} u_1 \\ u_2 \end{array} \right\} \Rightarrow \underline{\epsilon} = \underline{L}u \quad (1)$$

2.3 The stress-strain relations

Considering an isotropic and homogeneous material subjected to uniaxial tensile stress, one can expect it to extend towards the axis direction and to contract transversally. In linear elasticity, stresses

are proportional to strains, being the Young's Modulus (E) the proportionality constant. The proportion of contraction relative to the normal extension is given by the Poisson ratio (ν) (DES-UA, 2015)

The abovementioned relation, also known as elasticity equation or Hooke's law, can be written as follows

$$\varepsilon_{11} = \frac{1}{E} \sigma_{11}, \quad \varepsilon_{22} = \varepsilon_{33} = -\frac{\nu}{E} \sigma_{11} \quad (2)$$

For a 3D equilibrium the constitutive equations are presented in Figure 2.3a., where the elasticity matrix \underline{D} , for isotropic materials, is expressed in terms of E and ν (the shear modulus is

$$G = \frac{E}{2(1+\nu)}).$$

When considering the cases of plane stress or plane strain, the constitutive equations can be simplified as is presented in Figure 2.3b.

2.4 Equilibrium equation. The relation between stress spatial derivatives and body forces

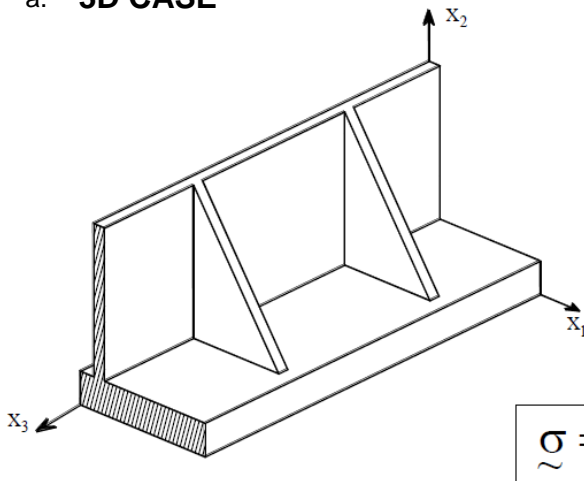
In Figure 2.4 is shown the equilibrium, in x_1 direction, of a 2D infinitesimal material element (a quadrilateral element of area $dx_1 dx_2$) considering the stress spatial variation and the resultant forces at the infinitesimal sides. In the figure, f_1 represents the body force in x_1 direction. It is relevant to note that f_1 could represent gravitational forces as well as inertial and damping forces.

The equilibrium equation for 2D case is

$$\begin{cases} \sum F_{x_1} = 0 \Rightarrow \frac{\partial \sigma_{11}}{\partial x_1} + \frac{\partial \sigma_{21}}{\partial x_2} + f_1 = 0 \\ \sum F_{x_2} = 0 \Rightarrow \frac{\partial \sigma_{12}}{\partial x_1} + \frac{\partial \sigma_{22}}{\partial x_2} + f_2 = 0 \end{cases} \Rightarrow \quad (5)$$

$$\Rightarrow \begin{bmatrix} \frac{\partial}{\partial x_1} & 0 & \frac{\partial}{\partial x_2} \\ 0 & \frac{\partial}{\partial x_2} & \frac{\partial}{\partial x_1} \end{bmatrix} \begin{Bmatrix} \sigma_{11} \\ \sigma_{22} \\ \sigma_{12} \end{Bmatrix} + \begin{Bmatrix} f_1 \\ f_2 \end{Bmatrix} = \begin{Bmatrix} 0 \\ 0 \end{Bmatrix} \Rightarrow \quad \underline{L}^T \underline{\sigma} + \underline{f} = \underline{0}$$

a. 3D CASE



$$\begin{bmatrix} \sigma_{11} \\ \sigma_{22} \\ \sigma_{33} \\ \sigma_{23} \\ \sigma_{31} \\ \sigma_{12} \end{bmatrix} = \begin{bmatrix} \frac{E(1-\nu)}{(1+\nu)(1-2\nu)} & \frac{E\nu}{(1+\nu)(1-2\nu)} & \frac{E\nu}{(1+\nu)(1-2\nu)} & 0 & 0 & 0 \\ & \frac{E(1-\nu)}{(1+\nu)(1-2\nu)} & \frac{E\nu}{(1+\nu)(1-2\nu)} & 0 & 0 & 0 \\ & & \frac{E(1-\nu)}{(1+\nu)(1-2\nu)} & 0 & 0 & 0 \\ 0 & 0 & 0 & G & 0 & 0 \\ 0 & 0 & 0 & 0 & G & 0 \\ 0 & 0 & 0 & 0 & 0 & G \end{bmatrix} \begin{bmatrix} \epsilon_{11} \\ \epsilon_{22} \\ \epsilon_{33} \\ 2\epsilon_{23} \\ 2\epsilon_{31} \\ 2\epsilon_{12} \end{bmatrix}$$

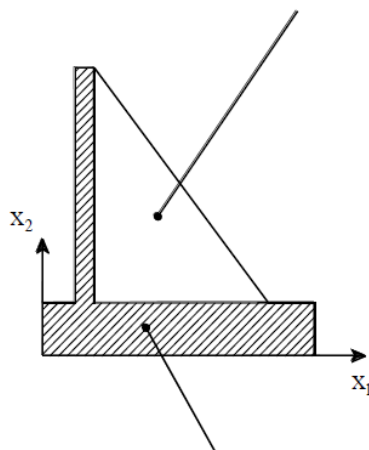
$\underline{\sigma} = \underline{D} \underline{\epsilon}$

$\underline{D}_{(6 \times 6)}$ Elasticity matrix for general 3D case

b. 2D CASE

$\sigma_{33} = 0 \quad \sigma_{23} = \sigma_{31} = 0$

Plane stress



$$\begin{bmatrix} \sigma_{11} \\ \sigma_{22} \\ \sigma_{12} \end{bmatrix} = \begin{bmatrix} \frac{E}{(1-\nu^2)} & \frac{\nu E}{(1-\nu^2)} & 0 \\ \frac{\nu E}{(1-\nu^2)} & \frac{E}{(1-\nu^2)} & 0 \\ 0 & 0 & \frac{E}{2(1+\nu)} \end{bmatrix} \begin{bmatrix} \epsilon_{11} \\ \epsilon_{22} \\ 2\epsilon_{12} \end{bmatrix}$$

$\underline{D}_{(3 \times 3)}$ Elasticity matrix for plane stress

$\epsilon_{33} = -\frac{\nu}{E} (\sigma_{11} + \sigma_{22})$

Plane strain

$\epsilon_{33} = 0 \quad \epsilon_{23} = \epsilon_{31} = 0$

$$\begin{bmatrix} \sigma_{11} \\ \sigma_{22} \\ \sigma_{12} \end{bmatrix} = \begin{bmatrix} \frac{E(1-\nu)}{(1+\nu)(1-2\nu)} & \frac{E\nu}{(1+\nu)(1-2\nu)} & 0 \\ \frac{E\nu}{(1+\nu)(1-2\nu)} & \frac{E(1-\nu)}{(1+\nu)(1-2\nu)} & 0 \\ 0 & 0 & \frac{E}{2(1+\nu)} \end{bmatrix} \begin{bmatrix} \epsilon_{11} \\ \epsilon_{22} \\ 2\epsilon_{12} \end{bmatrix}$$

$\underline{D}_{(3 \times 3)}$ Elasticity matrix for plane strain

$\sigma_{33} = \frac{E\nu}{(1+\nu)(1-2\nu)} (\epsilon_{11} + \epsilon_{22})$

Figure 2.3 – Constitutive equations. 3D and 2D cases. Plane strain and plane stress (adapted from Oliveira, S., 2016)

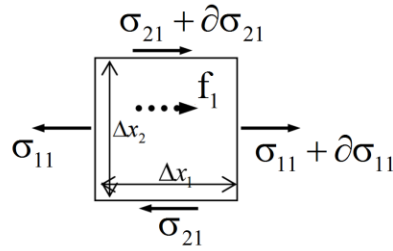


Figure 2.4 – Body forces, normal and shear stresses acting on a differential element (adapted from DES-UA, 2008)

2.5 Navier's equation

In Figure 2.5 it can be noticed that it is possible to replace $\underline{\varepsilon}$ by $\underline{L}u$ in the elasticity equation and that $\underline{D}u$ can replace $\underline{\sigma}$ in the equilibrium equation. So it results the Navier's equation, which is a fundamental equation of solid mechanics (displacement formulation). The Navier's equation establishes a relation between body forces and displacement derivatives.

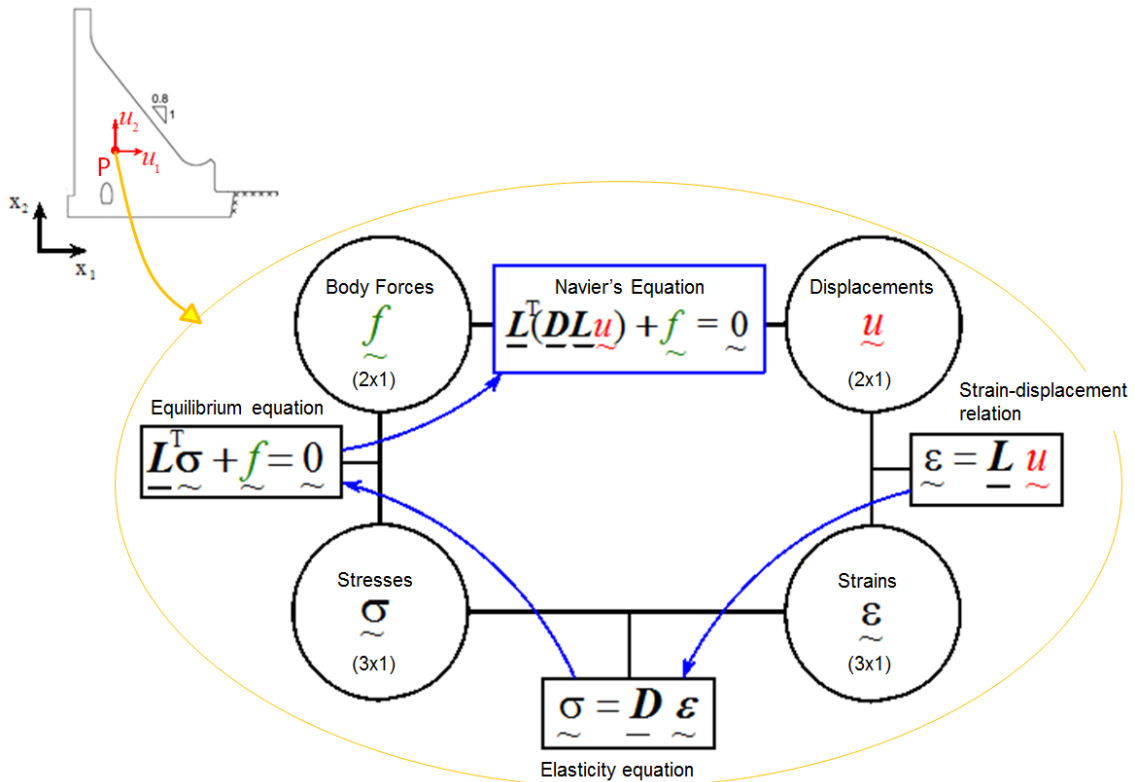


Figure 2.5 – Main equations of Solid Mechanics (adapted from Oliveira, S., 2016)

For engineering structures it is not possible to solve analytically the correspondent boundary values problem involving the Navier equation (differential equation with second order partial derivatives), consequently, it is necessary the use of numerical methods like the FEM.

In the next section it is briefly explained how the Navier's equation (differential equation, or strong form) can be transformed into an integral equation (weak form), used for obtaining the numerical solution by FEM.

2.6 Weak formulation

As referred above, in order to achieve numerical solutions for Navier's differential equation using the FEM, it is convenient to find an integral form (weak form) of the equation $\underline{L}^T(\underline{D}\underline{L}u) + \underline{f} = \underline{0}$, which is a differential equation, of the general form $F(x)=0$, that should be verified in the domain (structure's volume) for some predefined boundary conditions. Through the application of the Fundamental Lemma of Calculus of Variations (FLCV), which is the basis of the weighted residual method, function $F(x)$ is zero in its domain if the integral of $F(x)$ multiplied by any trial function $\underline{v} = \underline{v}(x)$ is equal to zero (eq.6)

$$F(x) = 0, x \in V \Leftrightarrow \int_V F(x) \underline{v}(x) dx = 0, \text{ for any trial function } \underline{v}(x) \in C_V^\infty \quad (6)$$

Consequently,

$$\left\{ \begin{array}{l} \int_V \underline{v}^T \cdot [\underline{L}^T(\underline{D}\underline{L}u) + \underline{f}] dV = 0, \forall \underline{v} \in C_V^\infty \\ \text{Boundary Conditions} \end{array} \right. \quad (7)$$

Using the Green-Gauss theorem, equation 7 becomes,

$$\int_V (\underline{L}\underline{v})^T \underline{D}\underline{L}u dV = \int_V \underline{v}^T \underline{f} dV, \forall \underline{v} \in C_V^\infty \quad (8)$$

There are three last notes which deserve mentioning. Firstly, it is noticeable that equation 8 is free of second order derivatives. There are only first order partial derivatives from the unknown function u . Secondly, it is important to remind that one can directly deduce the integral form of Navier's Equation by applying the Principle of Virtual Works (PVW). Finally, the trial functions (\underline{v}) correspond to the concept of virtual displacement field used in the PVW.

3 | Finite Element Method

3.1 Introductory considerations

In structural analysis, the numerical solution of the boundary value problem involving the Navier's equation is usually performed using a discretization into finite elements (FE). The structure is divided into elements of finite volume (FE), connected with each other by nodal points. The goal is to compute the displacement vectors at the nodal points considered.

The FEM's main idea is to consider that the displacement field $\underline{u} = \underline{u}(x_1, x_2, x_3)$ may be achieved through a linear combination of interpolation functions or shape functions \underline{N} . At a given point P within a finite element, the displacement vector \underline{u}_p can be obtained using the values \underline{N}_p of the interpolation functions in P, and the values of the element nodal displacements (\underline{u}^e): $\underline{u}_p = \underline{N}_p \underline{u}^e$. It should be noticed that \underline{u}^e is a column vector with the displacement values at the element nodal points.

For a 2D quadrilateral element of 4 nodes, \underline{u}_p becomes:

$$\underline{u} = \underline{N} \underline{u}^e \Rightarrow \begin{Bmatrix} u_1 \\ u_2 \end{Bmatrix} = \begin{bmatrix} N_1 & 0 & N_2 & 0 & N_3 & 0 & N_4 & 0 \\ 0 & N_1 & 0 & N_2 & 0 & N_3 & 0 & N_4 \end{bmatrix} \begin{Bmatrix} \underline{u}_1^{e,1} \\ \underline{u}_2^{e,1} \\ \underline{u}_1^{e,2} \\ \underline{u}_2^{e,2} \\ \underline{u}_1^{e,3} \\ \underline{u}_2^{e,3} \\ \underline{u}_1^{e,4} \\ \underline{u}_2^{e,4} \end{Bmatrix} \quad (9)$$

For a 2D quadrilateral element of 9 nodes we have

$$\underline{u} = \underline{N} \underline{u}^e \Rightarrow \begin{Bmatrix} u_1 \\ u_2 \end{Bmatrix} = \begin{bmatrix} N_1 & 0 & N_2 & 0 & \dots & N_9 & 0 \\ 0 & N_1 & 0 & N_2 & \dots & 0 & N_9 \end{bmatrix} \begin{Bmatrix} \underline{u}_1^{e,1} \\ \underline{u}_2^{e,1} \\ \underline{u}_1^{e,2} \\ \underline{u}_2^{e,2} \\ \vdots \\ \underline{u}_1^{e,9} \\ \underline{u}_2^{e,9} \end{Bmatrix} \quad (10)$$

Considering that the virtual displacement field within a finite element can be reached by an expression identical to 10, it results

$$\underline{v} = \underline{N} \underline{v}^e \quad (11)$$

Hence, the weak form of Navier's equation can be written as follows, for a finite element of volume V_e , considering expressions 8, 9, 10 and 11.

$$\int_{V_e} [\underline{\underline{L}}(\underline{\underline{N}}\underline{\underline{u}}^e)]^T \underline{\underline{D}}\underline{\underline{L}}(\underline{\underline{N}}\underline{\underline{u}}^e) dV = \int_{V_e} (\underline{\underline{N}}\underline{\underline{u}}^e)^T \underline{\underline{f}} dV, \quad \forall \underline{\underline{u}} = \underline{\underline{N}}\underline{\underline{u}}^e \quad (12)$$

Simplifying, by elimination of $\underline{\underline{u}}^e$, we obtain

$$\int_{V_e} (\underline{\underline{L}}\underline{\underline{N}})^T \underline{\underline{D}}(\underline{\underline{L}}\underline{\underline{N}}) dV \quad \underline{\underline{u}}^e = \int_{V_e} \underline{\underline{N}}^T \underline{\underline{f}} dV \quad (13)$$

Using the notation $\underline{\underline{B}} = \underline{\underline{L}}\underline{\underline{N}}$ for the derivatives of the interpolation functions (Zienkiewicz et al., 2005), we can write

$$\int_{V_e} \underline{\underline{B}}^T \underline{\underline{D}}\underline{\underline{B}} dV \quad \underline{\underline{u}}^e = \int_{V_e} \underline{\underline{N}}^T \underline{\underline{f}} dV \quad (14)$$

or

$$\underline{\underline{K}}^e \quad \underline{\underline{u}}^e = \quad \underline{\underline{F}}^e \quad (15)$$

that is known as the equilibrium equation of a finite element, in the algebraic form, where,

$$\underline{\underline{K}}^e = \int_{V_e} \underline{\underline{B}}^T \underline{\underline{D}}\underline{\underline{B}} dV \text{ - Finite element stiffness matrix.}$$

$$\underline{\underline{F}}^e = \int_{V_e} \underline{\underline{N}}^T \underline{\underline{f}} dV \text{ - Finite element nodal forces vector.}$$

Figure 3.1 schematically presents how it is possible to discretize a structure in finite elements and how to introduce FEM's fundamental approximation in Navier's equation weak form in order to obtain the equilibrium equations in the algebraic form.

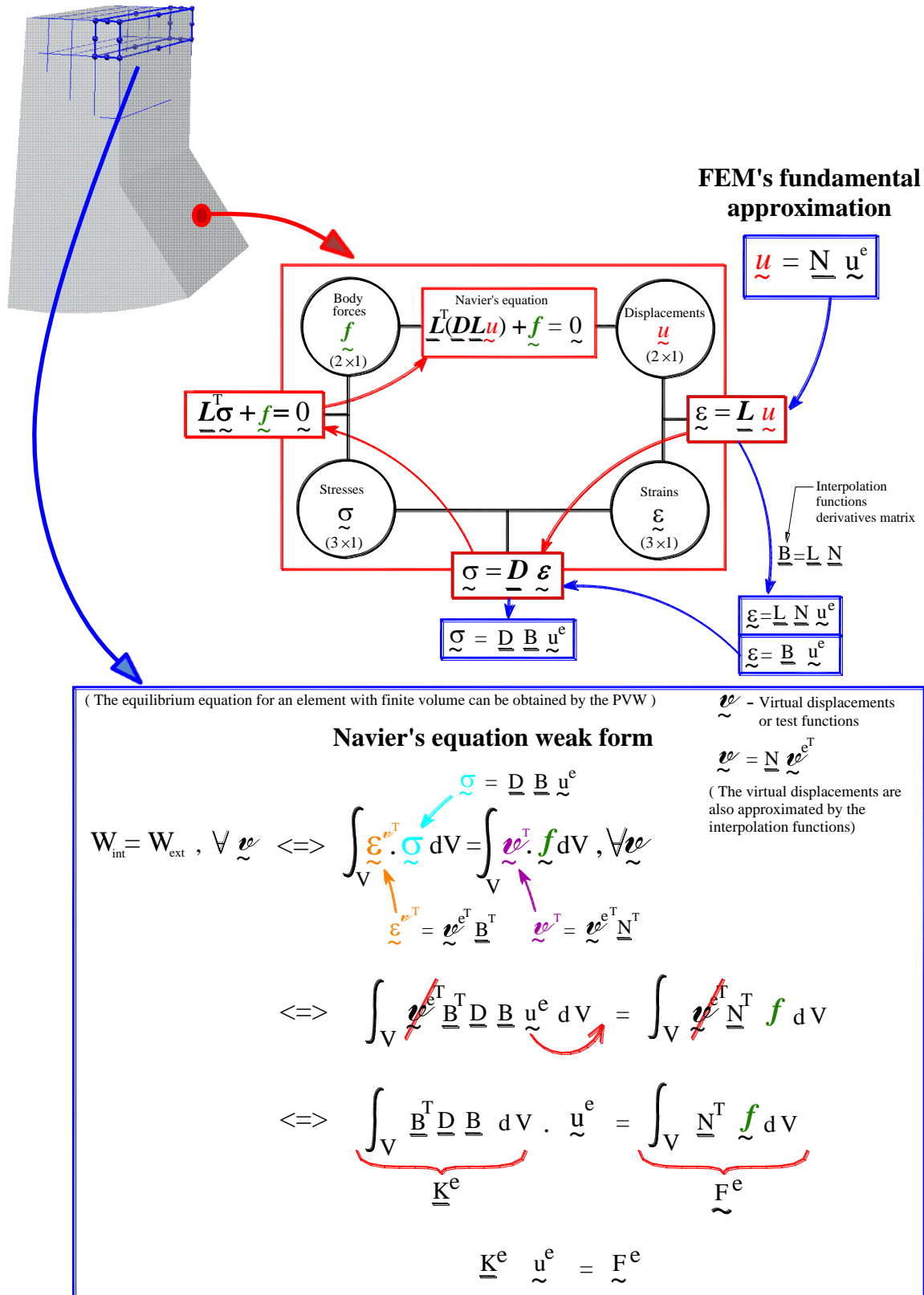


Figure 3.1 – Structural analysis using FEM. Introduction of FEM's fundamental approximation in the integral form of Navier's equation

3.2 Finite element with 4 nodal points for plane structures

For this study, considering 2D equilibria, it was decided to use a master isoparametric Lagrangian element of the type linear with 4 nodal points and another one of the type quadratic with 9 nodal points. In this sub-chapter is presented the 4 nodal points master element.

Figure 3.2 presents the notation used for local axis (y_1 and y_2), the local degrees of freedom (from $u_1^{e,1}$ to $u_2^{e,4}$), the nodes (from N1 to N4) and the Gaussian interpolation points (red crosses).

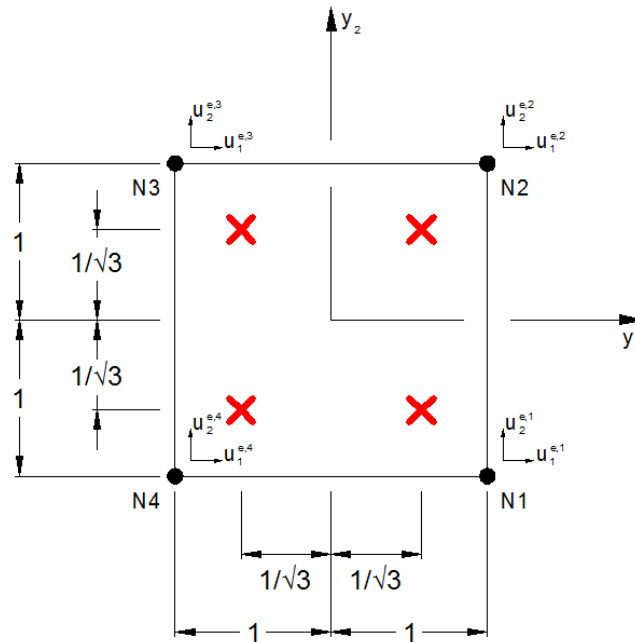


Figure 3.2 – Plain, 4 nodes, isoparametric finite element. The Gaussian interpolation points locations are presented with the red color cross

The Gauss weights, for this 4 nodes element, are all equal to 1.¹

Equations 16 present the analytical expressions for the interpolation functions of each node. In Figure 3.3 the shape functions are presented.

$$\begin{cases} N_1 = 0.25 \times (1 + y_1) \times (1 - y_2) \\ N_2 = 0.25 \times (1 + y_1) \times (1 + y_2) \\ N_3 = 0.25 \times (1 - y_1) \times (1 + y_2) \\ N_4 = 0.25 \times (1 - y_1) \times (1 - y_2) \end{cases} \quad (16)$$

¹ The sum of all Gauss weights, for any 2D quadrangular master element, is equal to 4.

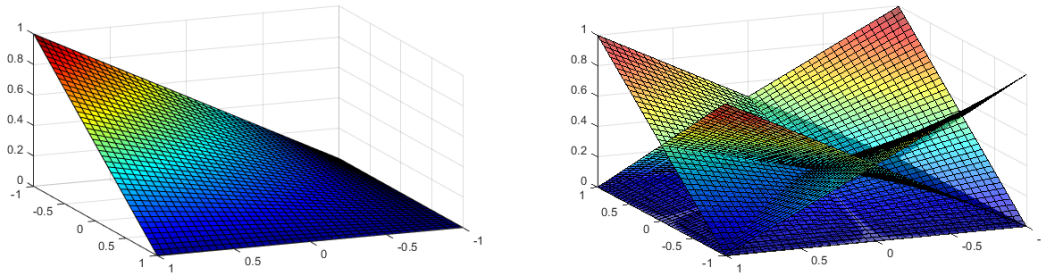


Figure 3.3 – Interpolation functions of the 4 nodal points element

3.3 2D finite element with 9 nodal points

Figure 3.4, presents the quadrilateral element with 9 nodal points. The location of Gauss points is presented and the correspondent weights (equal to $(5/9)^2$, $(8/9)^2$ and $5/9 \times 8/9$).

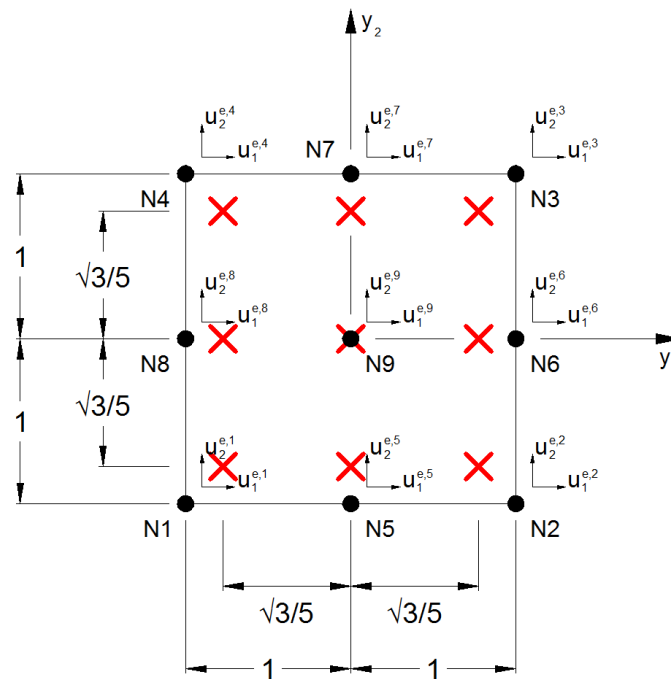


Figure 3.4 – Isoparametric finite element with 9 nodes (master). The Gauss interpolation points are represented with red color crosses

Equation (17) present the 9 analytical expressions for the interpolation functions (Figure 3.5).

$$\left. \begin{aligned}
 N_1 &= 0.25 \times (-1 + y_2) \times y_2 \times (-1 + y_1) \times y_1 \\
 N_2 &= 0.25 \times (-1 + y_2) \times y_2 \times (1 + y_1) \times y_1 \\
 N_3 &= 0.25 \times (1 + y_2) \times y_2 \times (1 + y_1) \times y_1 \\
 N_4 &= 0.25 \times (1 + y_2) \times y_2 \times (-1 + y_1) \times y_1 \\
 N_5 &= -(-1 + y_2) \times y_2 \times (-1 + y_1^2) \times 0.5 \\
 N_6 &= -(-1 + y_2^2) \times (1 + y_1) \times y_1 \times 0.5 \\
 N_7 &= -(1 + y_2) \times y_2 \times (-1 + y_1^2) \times 0.5 \\
 N_8 &= -(-1 + y_2^2) \times (-1 + y_1) \times y_1 \times 0.5 \\
 N_9 &= (-1 + y_2^2) \times (-1 + y_1^2)
 \end{aligned} \right\} \quad (17)$$

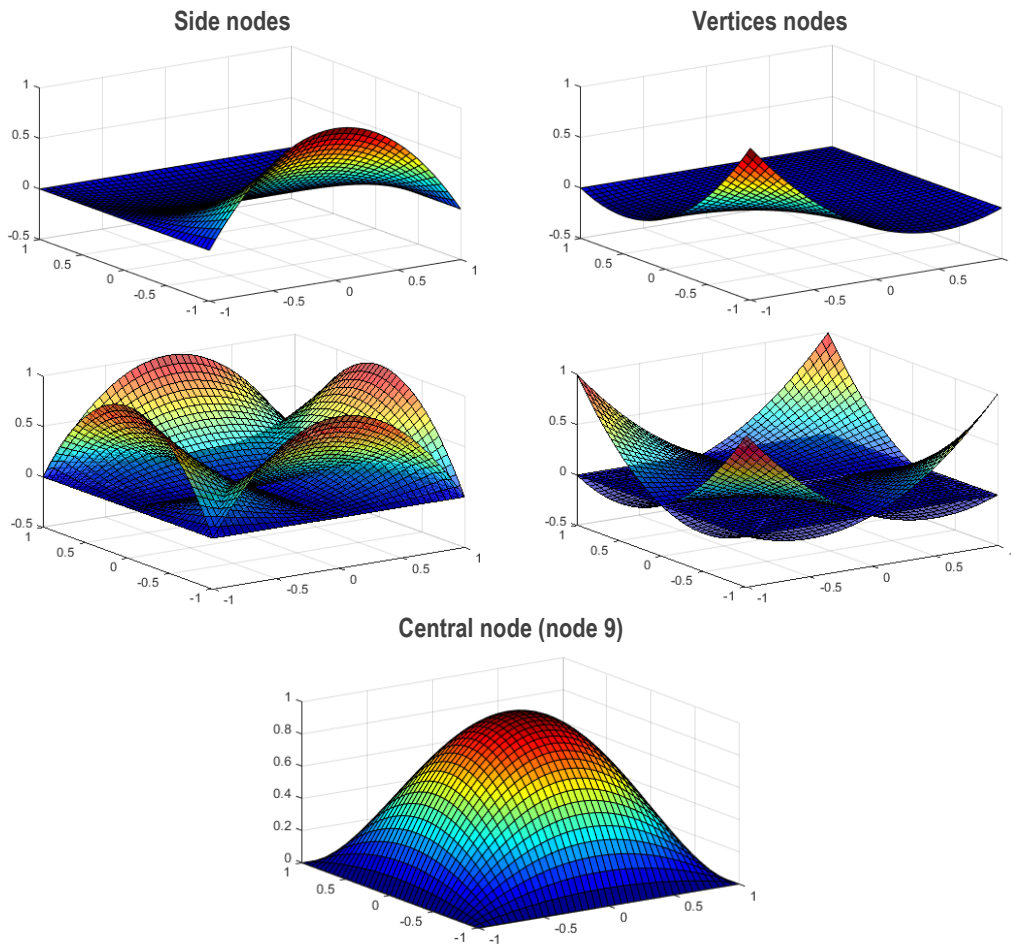


Figure 3.5 – Interpolation functions of the quadrilateral finite element with 9 nodal points

4 | The Program GDams2D 1.0

In this section are referred the main characteristics of the version 1.0 of the **GDams2D 1.0** program developed for 2D analysis of gravity dams using the finite element method (Figure 4.1). This initial version of the program is prepared to analyze the structural behavior of gravity dams for static loads, considering linear-elastic behavior, and using Lagrange finite elements of 4 sides, with 9 nodal points. The **GDams2D 1.0** program, developed in MATLAB, includes a module for automatic generation of meshes with a great level of refinement (generated from coarse meshes of quadrilaterals, with 4 nodal points at the vertices) and is designed for easy adaptation to non-linear analyzes, using stress-transfer modules such as those recently developed for the **DamSlide3D** and **DamDamage3D** programs.

For each finite element (**for n=1:NE**)

Calculate $\underline{x}_{(2 \times 4)} = \begin{bmatrix} x_1^{e_1} & x_1^{e_2} & x_1^{e_3} & x_1^{e_4} \\ x_2^{e_1} & x_2^{e_2} & x_2^{e_3} & x_2^{e_4} \end{bmatrix}$, element n nodes coordinates matrix

For each Gauss Point (**for iPG = 1: 4**) with local coordinates $y_1 = \pm 0.57735$, $y_2 = \pm 0.57735$

Calculate the Interpolation Function (IF) values and corresponding partial derivatives in respect to the local coordinates (in Gauss Point iPG):

$$\begin{aligned} N_1 &= \frac{1}{4}(1+y_1)(1-y_2) & \frac{\partial N_1}{\partial y_1} &= \frac{1}{4}(1-y_2) & \frac{\partial N_1}{\partial y_2} &= -\frac{1}{4}(1+y_1) \\ N_2 &= \frac{1}{4}(1+y_1)(1+y_2) & \frac{\partial N_2}{\partial y_1} &= \frac{1}{4}(1+y_2) & \frac{\partial N_2}{\partial y_2} &= \frac{1}{4}(1+y_1) \\ N_3 &= \frac{1}{4}(1-y_1)(1+y_2) & \frac{\partial N_3}{\partial y_1} &= -\frac{1}{4}(1+y_2) & \frac{\partial N_3}{\partial y_2} &= \frac{1}{4}(1-y_1) \\ N_4 &= \frac{1}{4}(1-y_1)(1-y_2) & \frac{\partial N_4}{\partial y_1} &= -\frac{1}{4}(1-y_2) & \frac{\partial N_4}{\partial y_2} &= -\frac{1}{4}(1-y_1) \end{aligned}$$

Calculate the Jacobian matrix:

$$\underline{J} = \begin{bmatrix} J_{11} & J_{12} \\ J_{21} & J_{22} \end{bmatrix} = \begin{bmatrix} x_1^{e_1} & x_1^{e_2} & x_1^{e_3} & x_1^{e_4} \\ x_2^{e_1} & x_2^{e_2} & x_2^{e_3} & x_2^{e_4} \end{bmatrix} \begin{bmatrix} \frac{\partial N_1}{\partial y_1} & \frac{\partial N_1}{\partial y_2} \\ \frac{\partial N_2}{\partial y_1} & \frac{\partial N_2}{\partial y_2} \\ \frac{\partial N_3}{\partial y_1} & \frac{\partial N_3}{\partial y_2} \\ \frac{\partial N_4}{\partial y_1} & \frac{\partial N_4}{\partial y_2} \end{bmatrix}$$

Calculate the IF partial derivatives in respect to the global coordinates:

$$\begin{bmatrix} \frac{\partial N_1}{\partial x_1} & \frac{\partial N_1}{\partial x_2} \\ \frac{\partial N_2}{\partial x_1} & \frac{\partial N_2}{\partial x_2} \\ \frac{\partial N_3}{\partial x_1} & \frac{\partial N_3}{\partial x_2} \\ \frac{\partial N_4}{\partial x_1} & \frac{\partial N_4}{\partial x_2} \end{bmatrix}_{PG} = \begin{bmatrix} \frac{\partial N_1}{\partial y_1} & \frac{\partial N_1}{\partial y_2} \\ \frac{\partial N_2}{\partial y_1} & \frac{\partial N_2}{\partial y_2} \\ \frac{\partial N_3}{\partial y_1} & \frac{\partial N_3}{\partial y_2} \\ \frac{\partial N_4}{\partial y_1} & \frac{\partial N_4}{\partial y_2} \end{bmatrix}_{PG} \cdot \underline{J}_{PG}^{-1}$$

Assemble matrix \underline{B} ($\underline{B} = \underline{L} \underline{N}$, $\underline{\varepsilon} = \underline{B} \underline{u}^e$)

$$\underline{B} = \begin{bmatrix} \frac{\partial N_1}{\partial x_1} & 0 & \frac{\partial N_2}{\partial x_1} & 0 & \frac{\partial N_3}{\partial x_1} & 0 & \frac{\partial N_4}{\partial x_1} & 0 \\ 0 & \frac{\partial N_1}{\partial x_2} & 0 & \frac{\partial N_2}{\partial x_2} & 0 & \frac{\partial N_3}{\partial x_2} & 0 & \frac{\partial N_4}{\partial x_2} \\ \frac{\partial N_1}{\partial x_2} & \frac{\partial N_1}{\partial x_1} & \frac{\partial N_2}{\partial x_2} & \frac{\partial N_2}{\partial x_1} & \frac{\partial N_3}{\partial x_2} & \frac{\partial N_3}{\partial x_1} & \frac{\partial N_4}{\partial x_2} & \frac{\partial N_4}{\partial x_1} \end{bmatrix}_{PG}$$

Calculate the matrix corresponding to the following matrix product:

$$t \underline{B}^T \underline{D} \underline{B} |\underline{J}|$$

(t - finite element thickness)

The numerical integration through the Gauss method for matrix $t \underline{B}^T \underline{D} \underline{B} |\underline{J}|$ over the finite element area (split in 4 quadrilaterals: one for each Gauss Point) is equal to the continuous sum of matrix $e \underline{B}^T \underline{D} \underline{B} |\underline{J}|$ for each Gauss Point (Gauss sum to obtain \underline{K}^e)

$$\underline{K}_{(8 \times 8)}^e = t \left(\underline{B}^T \underline{D} \underline{B} |\underline{J}| \right)_{PG1} + t \left(\underline{B}^T \underline{D} \underline{B} |\underline{J}| \right)_{PG2} + t \left(\underline{B}^T \underline{D} \underline{B} |\underline{J}| \right)_{PG3} + t \left(\underline{B}^T \underline{D} \underline{B} |\underline{J}| \right)_{PG4}$$

end

“Spreading” of the elementar matrices \underline{K}^e into the global stiffness matrix \underline{K} (assembly)

end

Figure 4.1 – MATLAB programming script scheme for the FEM elementar stiffness matrix calculus and subsequent assembly on the global stiffness matrix, considering a 4 nodal points 2D element

5 | Test Structures

5.1 Introductory considerations

The FEM numerical solutions should approach analytical solutions as the mesh is refined. Whether a p-refinement (polynomial refinement: in this section is made a comparison between results from a 4 nodes element mesh and from a 9 nodes element mesh) or an h-refinement (refinement in number of elements) are taken into consideration, it is always implied a convergence (DAES-UCB, 2017).

In order to verify the **GDams2D 1.0** basic structures were used, with known theoretical solutions

This chapter presents the results of the FEM's application to the following cases: a beam and a 2D plane elasticity structure.

5.2 2D structure

The first test case is about a 2D plane elasticity structure with its top and left face roller supported and with a constant distributed load applied on its bottom face (Figure 5.1). In this test, considering the plane stress hypothesis, it is expected $u_1 = -\nu \cdot u_2$.

In Figure 5.1 are presented results for a finite element mesh with linear quadrilateral elements of 4 nodes element. Figure 5.1a presents the structure's geometry, boundary conditions, applied forces, discretization and material properties. In Figure 5.1b and 5.1c. is presented the displacement field (components u_1 and u_2) and, finally, in Figure 5.1d is presented the stress field. In (b.), (c.) and (d.) are presented the results from FEM2D_4N, considering a master element with 4 nodes.

In Figure 5.2 are presented the same results for a finite element mesh with linear quadrilateral elements of 9 nodes element.

From Figure 5.1 and Figure 5.2 one can verify that the numerical results obtained with both discretizations corresponds to the theoretical results (for both displacement field and stress field).

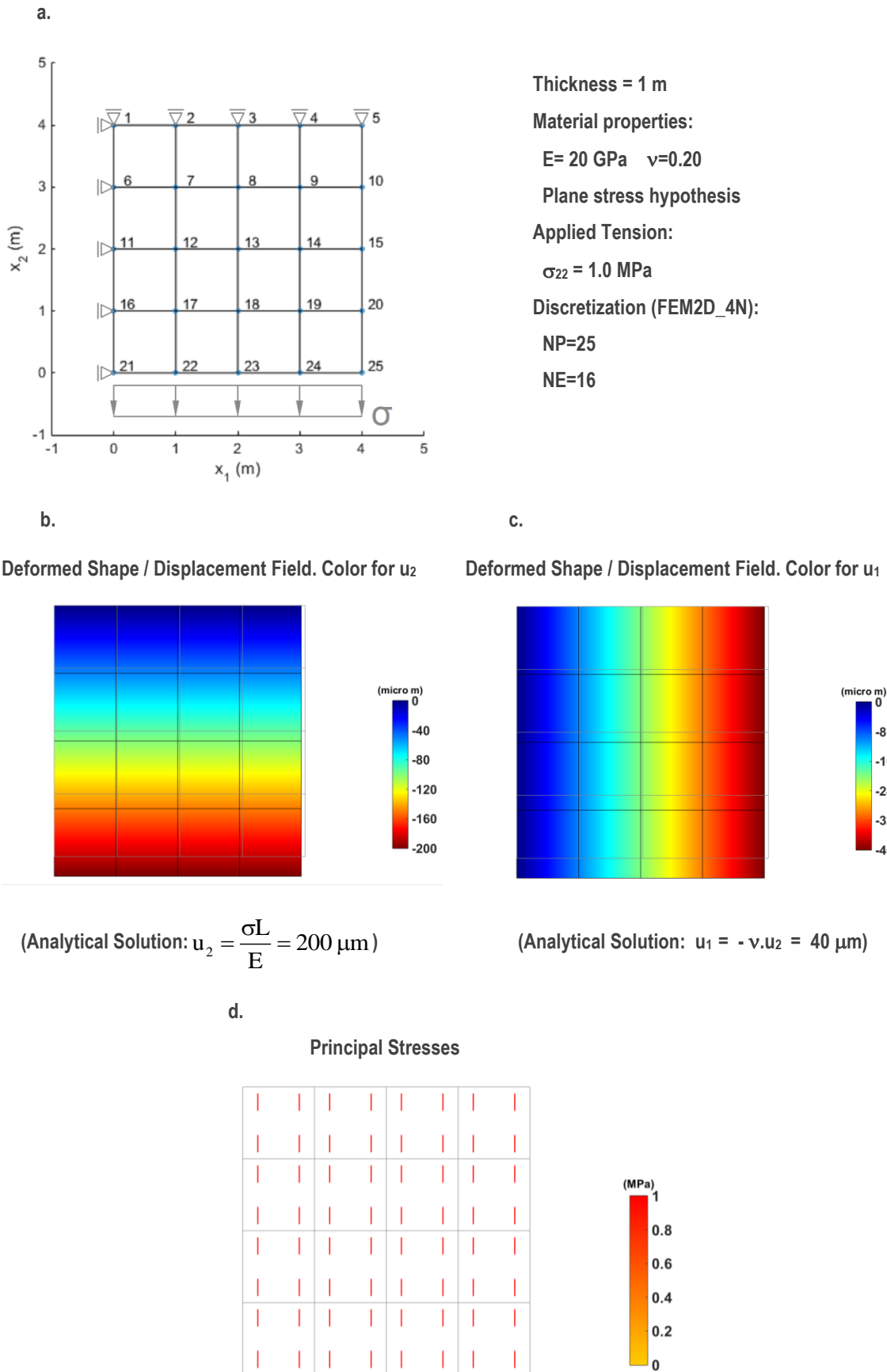


Figure 5.1 – Test example using a FE mesh with linear elements of 4 nodes (Plane elasticity)

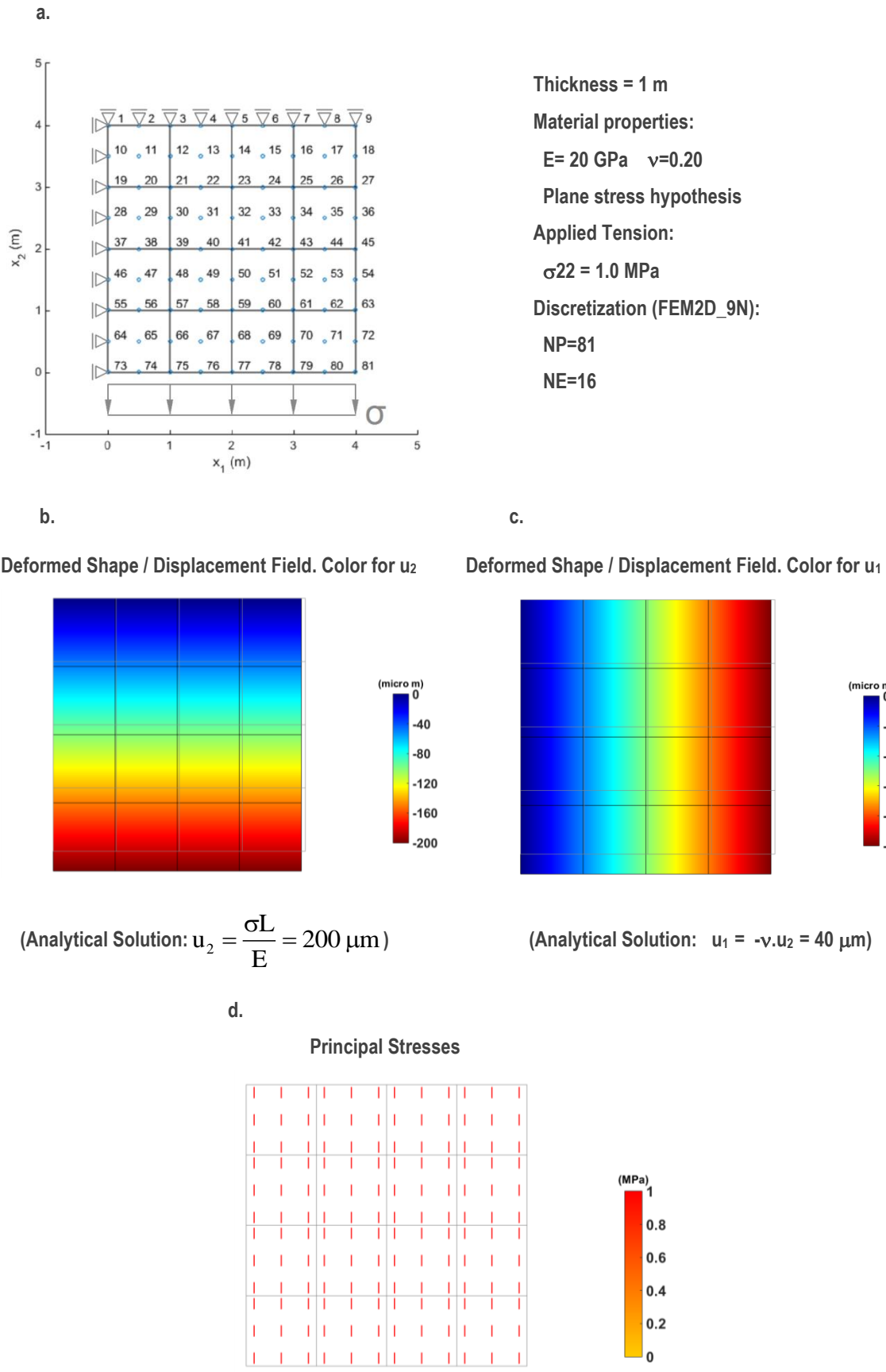


Figure 5.2 – Test example. Results from the program GDams2D1.0 (Plane elasticity)

When one centers the attention on the stresses fields presented in Figure 5.1d and in Figure 5.2d, it is possible to acknowledge that it emerges as expected. First, their values are evenly distributed across the structure and equal to the load/stress applied, which, in this case is 1 MPa. Secondly, the stresses are only generated under σ_{22} direction, the applied load direction, as a result, in the other direction (towards x_1 axis) the stresses are equal to zero. σ_{11} is equal to zero because the support conditions enables free movement for the deformation on the perpendicular direction. Since, there is no restrain to that movement, consequently, there are no stresses created under that direction as well.

From the analyses of the displacement fields along both x_1 and x_2 directions (Figure 5.1b, Figure 5.1c, Figure 5.2b and Figure 5.2c), and following exactly the purpose of the test, the relationship between displacements is equal to the Poisson's ratio. From the figures, the maximum displacement on node 25 is equal to $-200 \mu\text{m}$ under x_2 direction and $-40 \mu\text{m}$ under x_1 direction, which means that u_1 displacement is equal to u_2 displacement times the Poisson's coefficient, just as it was needed to be proved.

For the current loading, structure and support conditions, it is possible to calculate the theoretical maximum displacement by the following formula.

$$\begin{cases} u_2 = \frac{\sigma L}{E} = \frac{1 \times 10^6 \times 4 \times 10^6}{20 \times 10^9} = 200 \mu\text{m} \\ u_1 = -\nu u_2 = -0,2 \times 200 = -40 \mu\text{m} \end{cases} \quad (18)$$

This result is equal to those obtained numerically using both meshes, proving the outputs coherency for this test.

5.3 Fixed-fixed supported beam

In this section is considered a fixed-fixed beam, 10 m span, with rectangular section ($1 \times 1 \text{ m}$), subjected to the self-weight ($\gamma=25 \text{ kN/m}^3$). It was assumed the hypothesis of plane stress, with $E=20 \text{ GPa}$ and $\nu=0,2$. The beam displacements and principal stresses were numerically computed by FEM using two discretizations with linear FE of 4 nodes (Figs. 5.3 and 5.4) and two discretizations with 2nd order FE of 9 nodes used in **GDams2D** (Figs.5.5 and 5.6).

In what concerns the analytical solution, the maximum displacement at the center of the beam, considering shear deformation, is given by equation 19 (Ghugal, Y., Sharma, R., 2011).

$$\begin{aligned} u_{\frac{1}{2}\text{span}} &= \frac{qL^4}{384EI} \left[1 + 9.6(1+\nu) \frac{h^2}{L^2} \right] = \\ &= \frac{25 \times 10^4}{384 \times 20 \times 10^6 \times \frac{1 \times 1^3}{12}} \left[1 + 9.6(1+0.2) \times \frac{1^2}{10^2} \right] \times 10^6 = 435.63 \mu\text{m} \end{aligned} \quad (19)$$

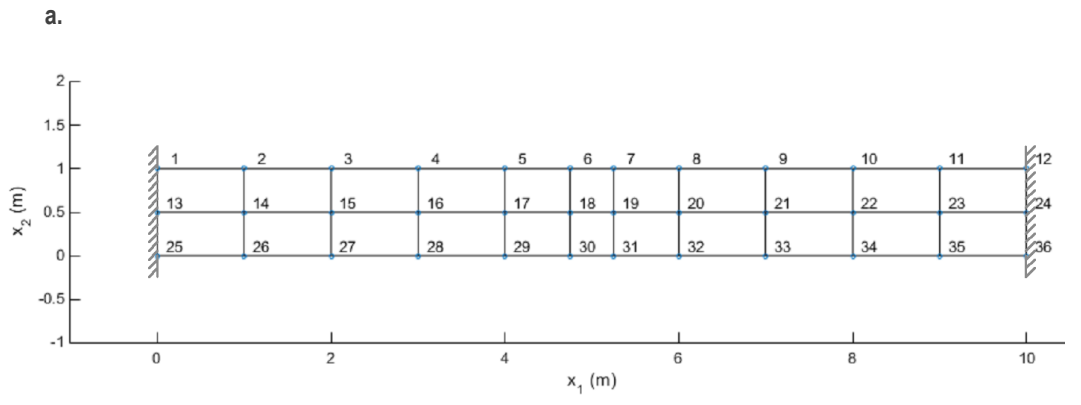
Using a coarse mesh with 22 finite elements of 4 nodes (FE4nodes) is computed a value of 314.33 μm for the middle span displacement (Figure 5.3), clearly lower than the theoretical value of 435.63 μm (a difference of about -27,85%). With this kind of linear elements it is necessary the use of a very "h" refined mesh in order to obtain a good result. Using a mesh with 5632 FE4nodes is computed a value of 433.68 μm for the middle span displacement (Figure 5.4), much closer to the theoretical value of 435.63 μm (a difference of about -0,45%).

On the other hand, using **GDams2D**, and a coarse mesh with 22 finite elements of 9 nodes (FE9nodes) the computed mid span displacement is 431.57 μm (Figure 5.5), close to the theoretical value of 435.63 μm (a difference of about -0,93%).

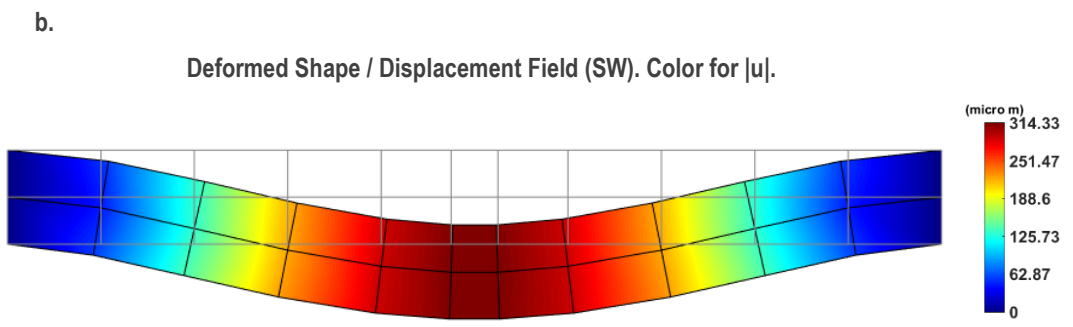
Also using **GDams2D**, and a very refined mesh, with 5632 FE9nodes, the computed mid span displacement is 434.41 μm (Figure 5.6), very close to the theoretical value of 435.63 μm (a difference of about -0,28%).

In what concerns the stresses it is also obtained a good agreement between computed and numerical results. For example, as presented in Figure 5.6c, the maximum tension stress at the mid span section should be 625 kPa (theoretical value: $\sigma_{\max} = M.y / I$, $M_{1/2} = qL^2 / 24$) and the numerical value obtained is 623,5 kPa (a small difference of about -0,24%).

In Figure 5.7 is shown how the numerical values computed for the mid span displacement, using meshes with increasing refinement, converge to the theoretical value.



Material properties:	Applied Load:	Discretization (FEM2D_4N):
E= 20 GPa	Self-Weight (SW) = 25 kN/m ³	NP=36
ν=0.20		NE=22
Plane stress hypothesis		



$$|u|_{l/2 \text{ span}} = \frac{qL^4}{384EI} \left[1 + 9.6(1 + \nu) \frac{h^2}{L^2} \right] = 435.63 \mu\text{m} \text{ (Ghugal, Y., Sharma, R., 2011)}$$

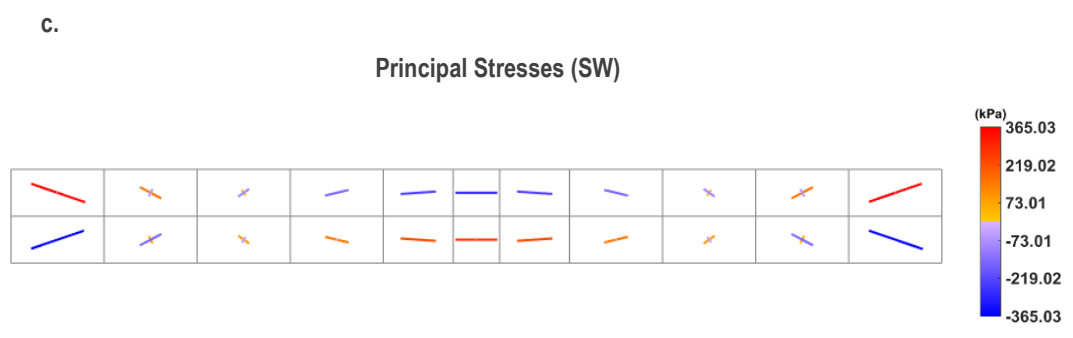


Figure 5.3 – Test example using a mesh with linear 4 node elements. Fixed-fixed beam: 22 elements discretization

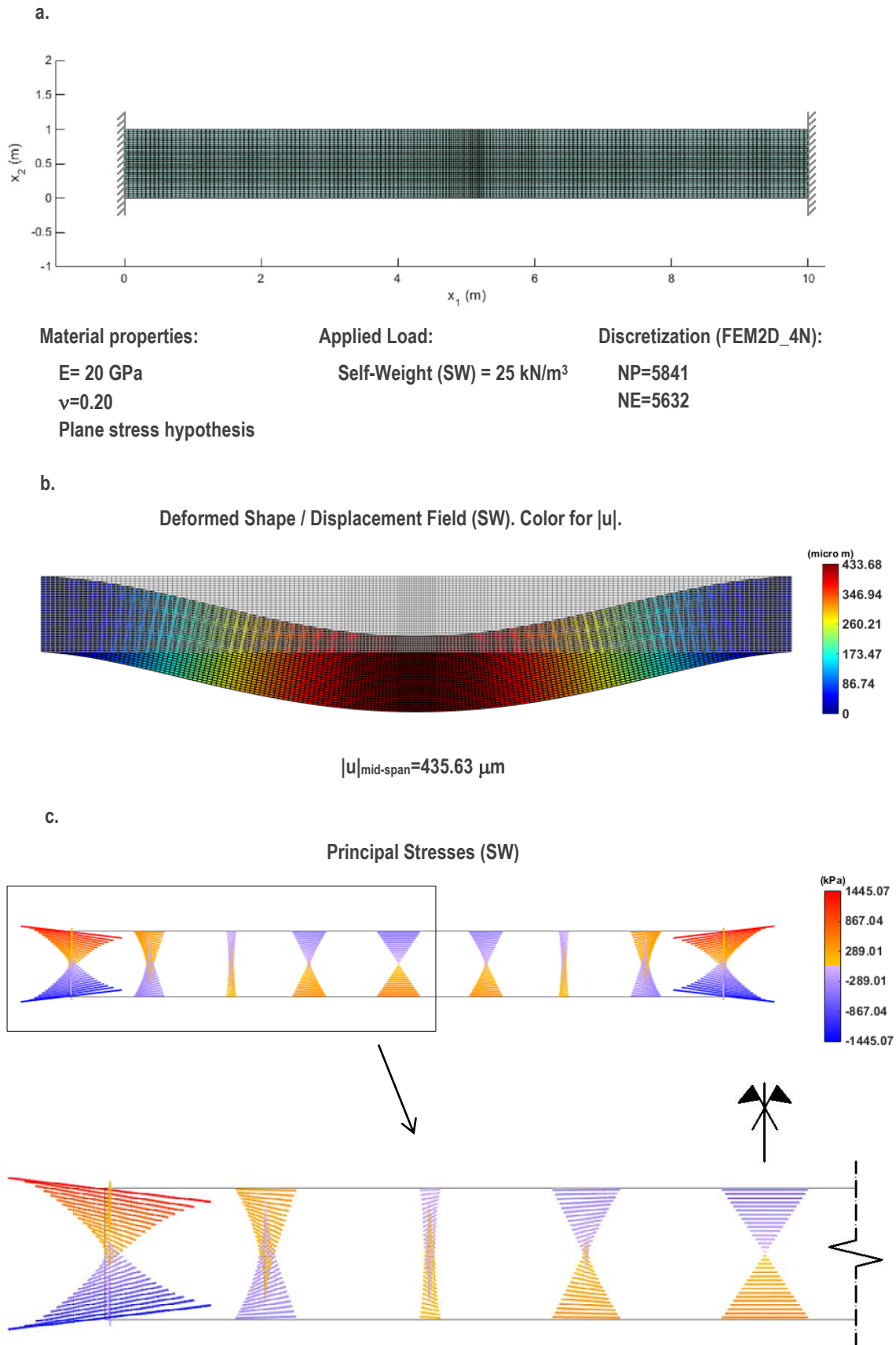
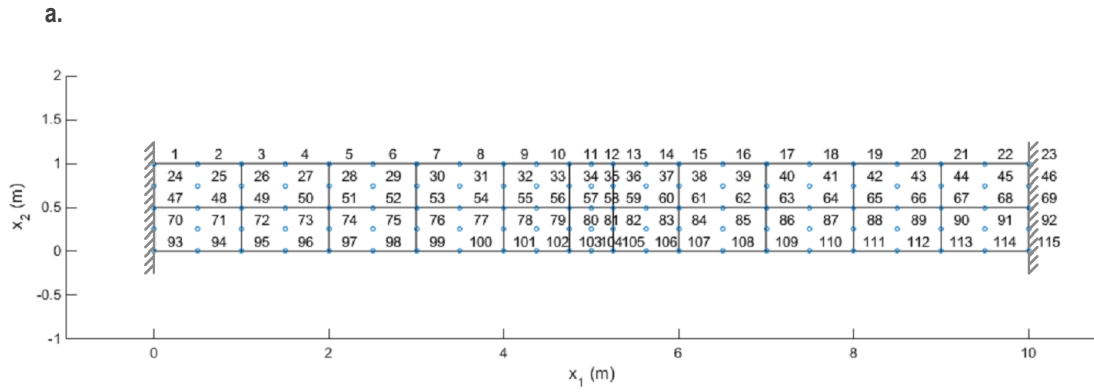


Figure 5.4 – Test example using a mesh with linear 4 node elements. Fixed-fixed beam. 5632 elements discretization



Material properties:

$E = 20 \text{ GPa}$
 $\nu = 0.20$
 Plane stress hypothesis

Applied Load:

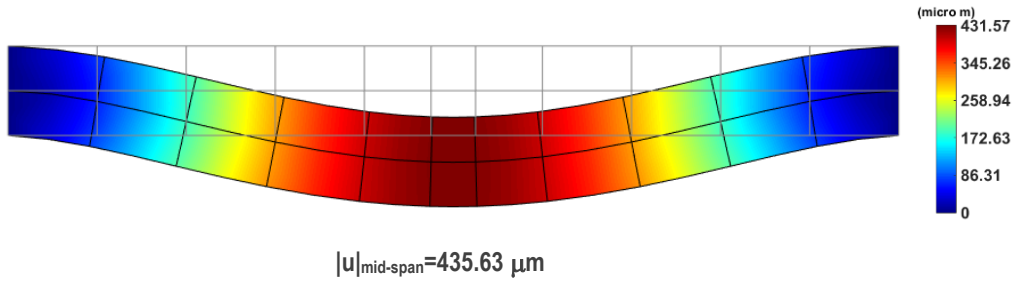
Self-Weight (SW) = 25 kN/m^3

Discretization (FEM2D_9N):

NP=115
 NE=22

b.

Deformed Shape / Displacement Field (SW). Color for $|u|$.



c.

Principal Stresses (SW)

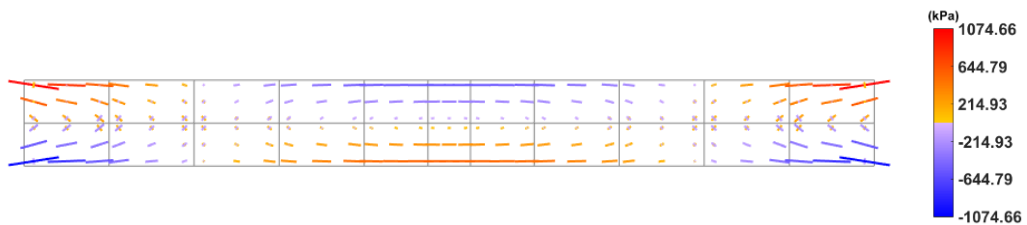


Figure 5.5 – Use of Lagrangian 2DFE of 9 nodes (GDams2D1.0). Fixed-fixed beam under SW load: coarse mesh with 22 elements. Displacements and principal stresses

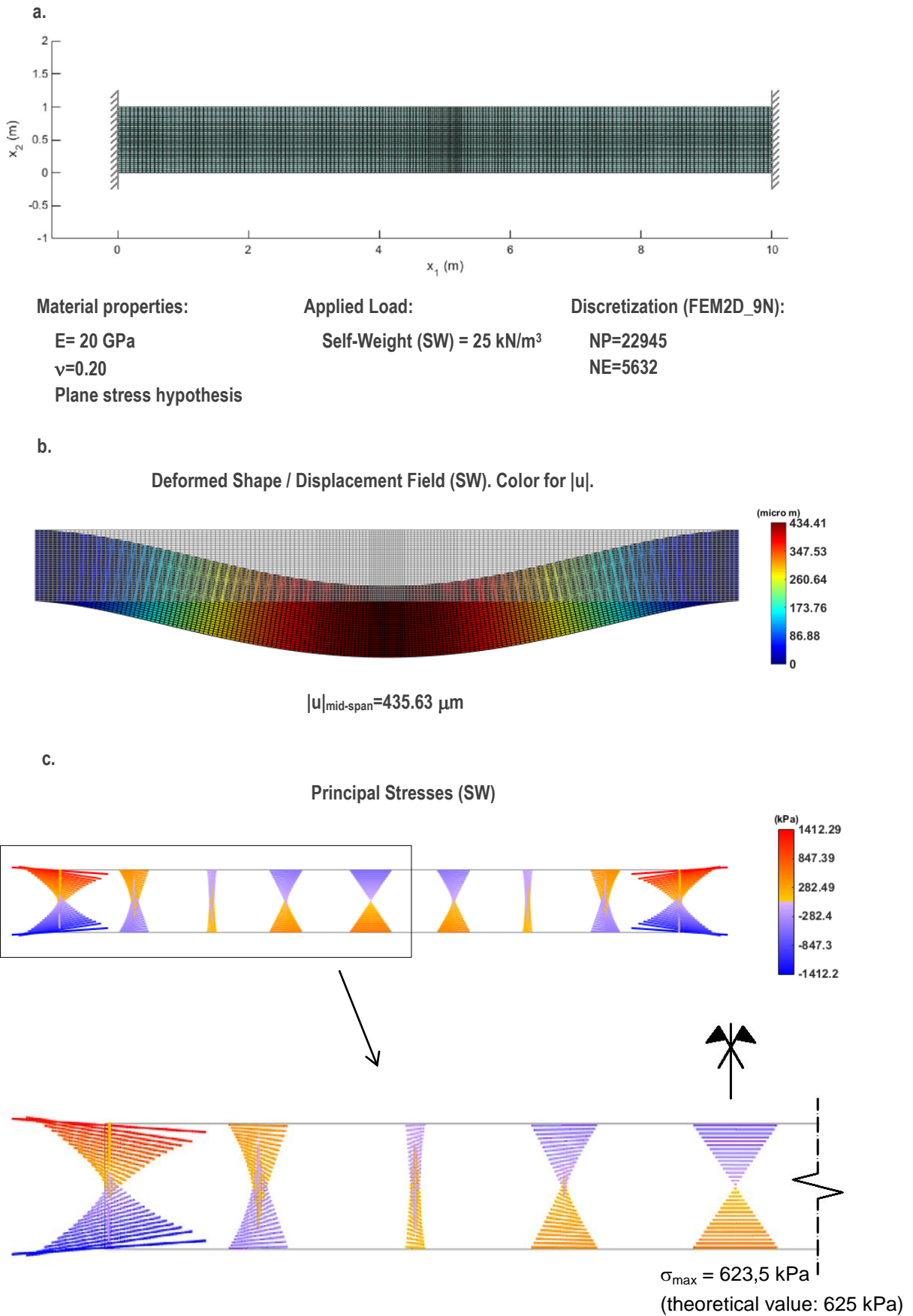


Figure 5.6 – Use of Lagrangian 2DFE of 9 nodes (GDams2D1.0). Fixed-fixed beam under SW load: fine mesh with 5632 elements (automatically generated with GDams2D1.0 from a coarse mesh). Displacements and principal stresses

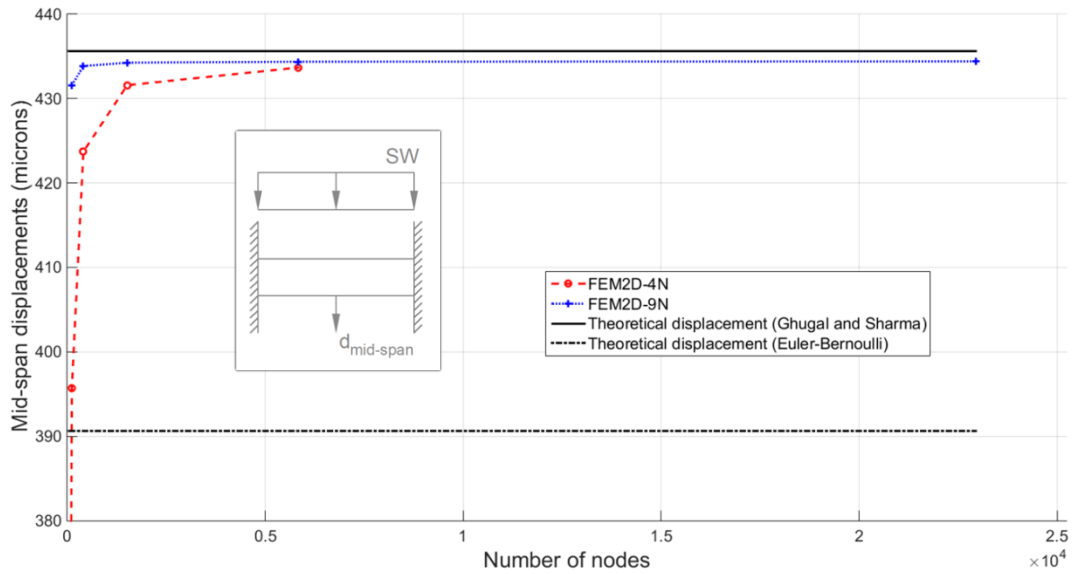


Figure 5.7 – Mid-span displacement on a fixed-fixed beam under SW load for different mesh refinements

5.3.1 Analysis of the stress patterns computed in each element

In FE computations using a displacement formulation, the stress distribution along sides of adjacent elements is not coherent. This implies that in elements with adjacent sides, only in some specific cases we will have a continuous distribution of the tension field across those referred adjacent sides. Although, it is important to underline that, at the limit, considering a continuous “h” and/or “p” refinement, the FEM will converge to the exact solution and, therefore, those element boundaries will have, at the limit, equal values (Zienkiewicz, O. C. et al., 2005). For example, Figure 5.8 presents the analysis of a cantilever beam formed by four rectangular serendipity elements with 8 nodes in which it is possible to understand how well the stresses sampled at the Gauss points (superconvergent points) behave when compared with the overall stress pattern computed in each element.

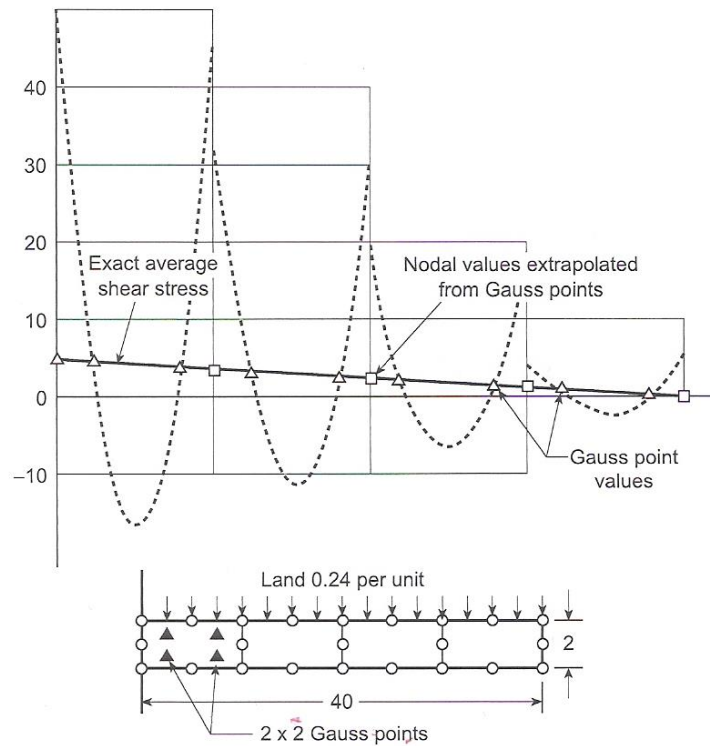


Figure 5.8 – Cantilever beam with four serendipity elements with 8 nodes. Stress sampling using 4 Gauss points (2x2) and extrapolation to nodes (Zienkiewicz, O. C. et al., 2005, p. 466) using the shape functions

In Figure 5.9 the numerical values of σ_{11} and σ_{12} computed in the fixed-fixed beam, with three different meshes of linear finite elements of 4nodes, are presented. It can be seen that for the normal component σ_{11} a good continuity between adjacent elements is obtained, namely for the most refined mesh. However, for the shear stress component σ_{12} it is not obtained a good continuity between adjacent elements.

In Figure 5.10 the numerical values of σ_{11} and σ_{12} computed with three different meshes of quadratic finite elements of 9nodes (**GDams2D**), are presented. It can be seen that for both stress components (σ_{11} and σ_{12}) a good continuity between adjacent elements is obtained, namely for the most refined mesh.

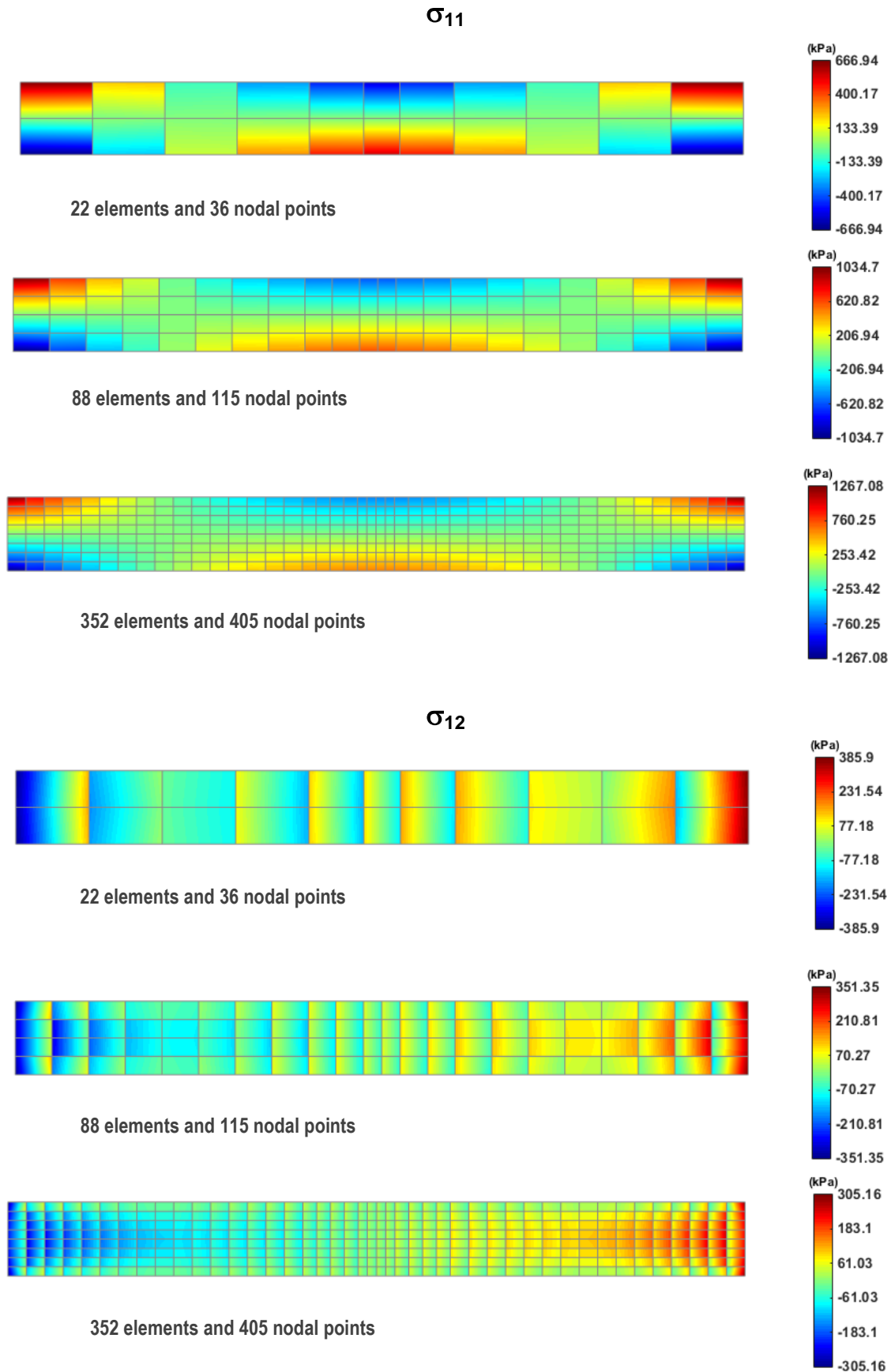


Figure 5.9 – Use of linear 2DFE with 4 nodes. Stress analysis: numerical results for σ_{11} and σ_{12} fields considering an increasing h-refinement in a fixed-fixed beam under the SW load

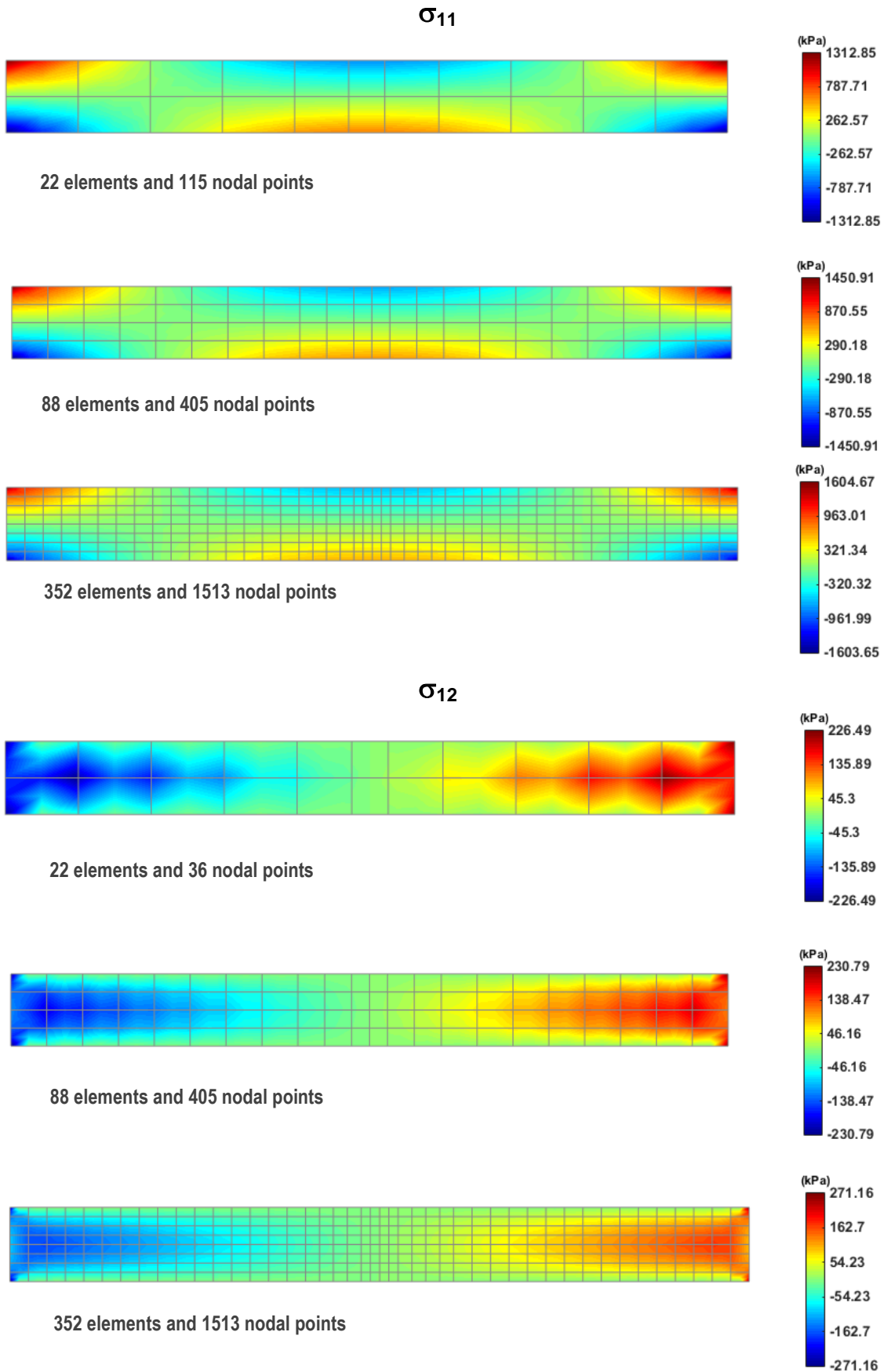


Figure 5.10 – Use of Lagrangian 2DFE of 9 nodes. Stress analysis (GDams2D1.0): numerical results for σ_{11} and σ_{12} fields considering an increasing h-refinement in a fixed-fixed beam under the SW load

6 | Gravity Dam. Case Study

6.1 Dam presentation

The case study here presented is a gravity dam, located in Ponsul's river (Tagus river basin), that was built for water supply and irrigation. The dam, in operation since 1978, is a 25 m high concrete gravity dam with a crest length of about 112 m (Figure 6.1).

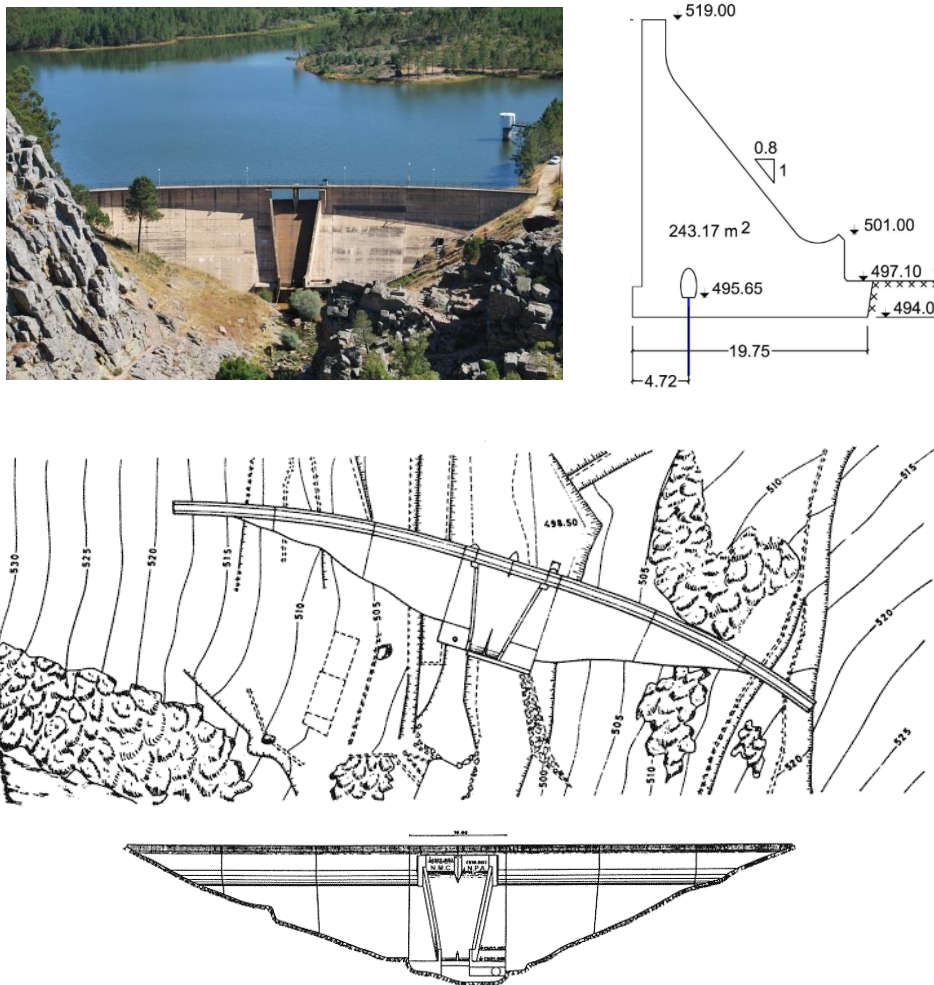


Figure 6.1 – Gravity dam. On the top left, downstream view (photo). On the top right, the cross section view (Pereira, R.; 2011). On the middle, the site plan. On the bottom, the downstream elevation view (CNPGB, 1992)

Taking advantage of the site topography and considering the plan view, the dam alignment presents a 16 m central straight section. Toward the sides, it reveals a circular geometry on the upstream face, which has a 150 m radius on the left river bank, and 160 m on the right bank. Both discharges (top

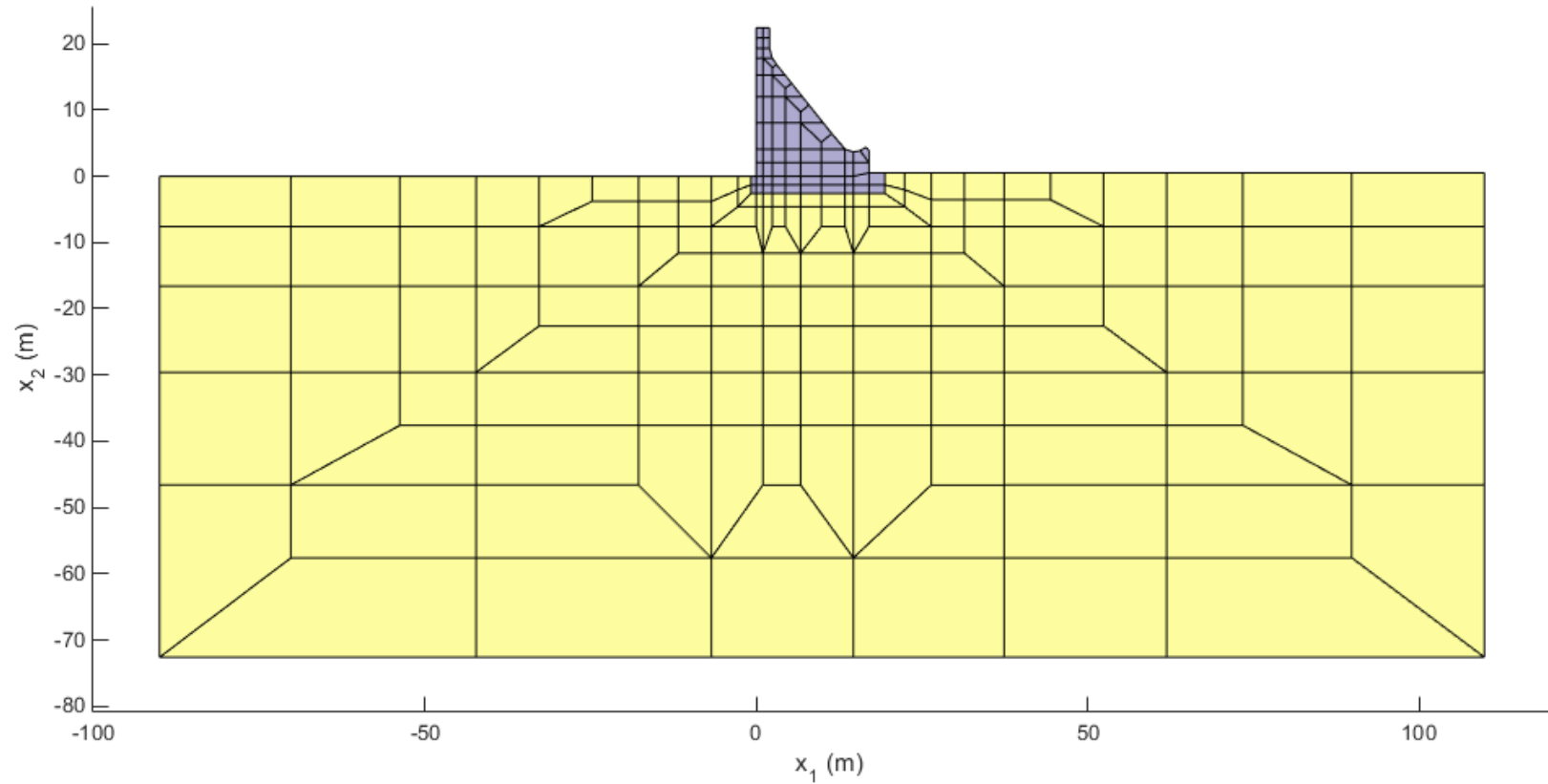
and bottom) are located on the central section. As a whole, the dam is composed by 7 blocks, 16 m each, split by watertight contraction joints. The concrete mixture used was composed by 250 kg of cement per cubic meter. A drainage/inspection gallery is located inside the dam's base and extends itself through most of the dam's length (top right of Figure 6.1). The dam has a triangular profile with a vertical upstream face and a $0.8H/1V$ inclined downstream face (AdC, 2009).

6.2 Dam structural behavior modelling

In order to study the dam structural behavior for the main loads, self-weight (SW) and hydrostatic pressure (HP) it was developed a 2D FE model of the dam central section (plane strain hypothesis). Using **GDams2D 1.0** it was considered an input mesh of FE4nodes, presented in Figure 6.2, that was automatically converted into a mesh of FE9nodes (Figure 6.3).

It was assumed for concrete an elasticity modulus $E_c = 30$ GPa and for the foundation $E_f = 20$ GPa. The Poisson ratio considered for both materials was $\nu=0.2$.

Figure 6.4 presents the displacements and principal stresses computed with **GDams2D1.0** for the self-weight (SW). Figure 6.5 present the same results for the hydrostatic pressure, considering full reservoir (HP_{FR}), and Figure 6.6 for the load combination $SW+HP_{FR}$. It should be noticed that for this load combination tension stresses do not occur at the upstream toe.



Material properties:

$E_{\text{concrete}} = 30 \text{ GPa}$; $E_{\text{foundation}} = 20 \text{ GPa}$; $\nu = 0.20$

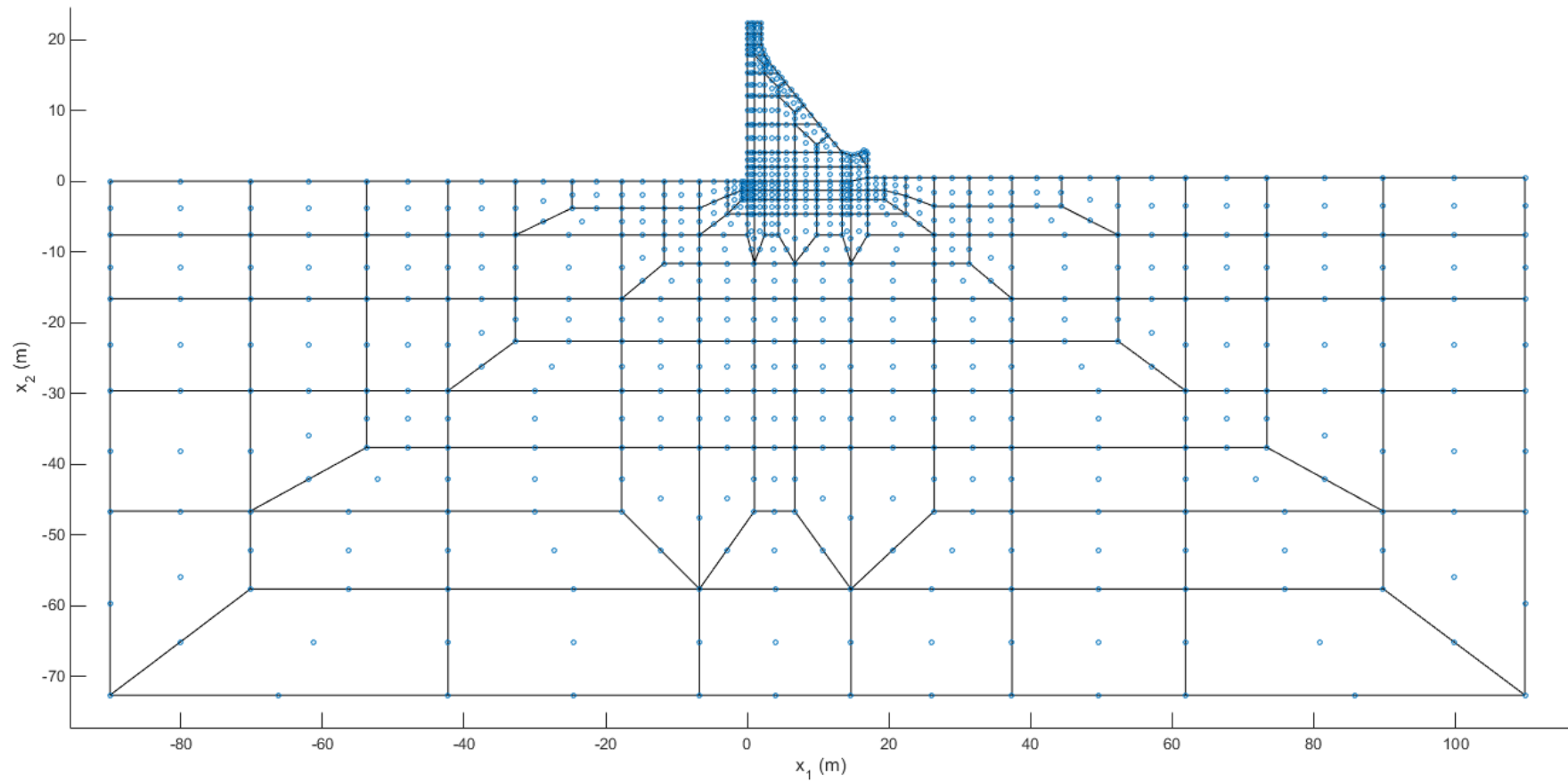
Plane strain hypothesis

Discretization (EF4N):

NP=235

NE=201

Figure 6.2 – Dam discretization. Input mesh (FE with 4 nodal points) used for automatic generation of the final mesh with Lagrangian FE of 9 nodes



Material properties:

$E_{\text{concrete}} = 30 \text{ GPa}$; $E_{\text{foundation}} = 20 \text{ GPa}$; $\nu = 0.20$

Plane strain hypothesis

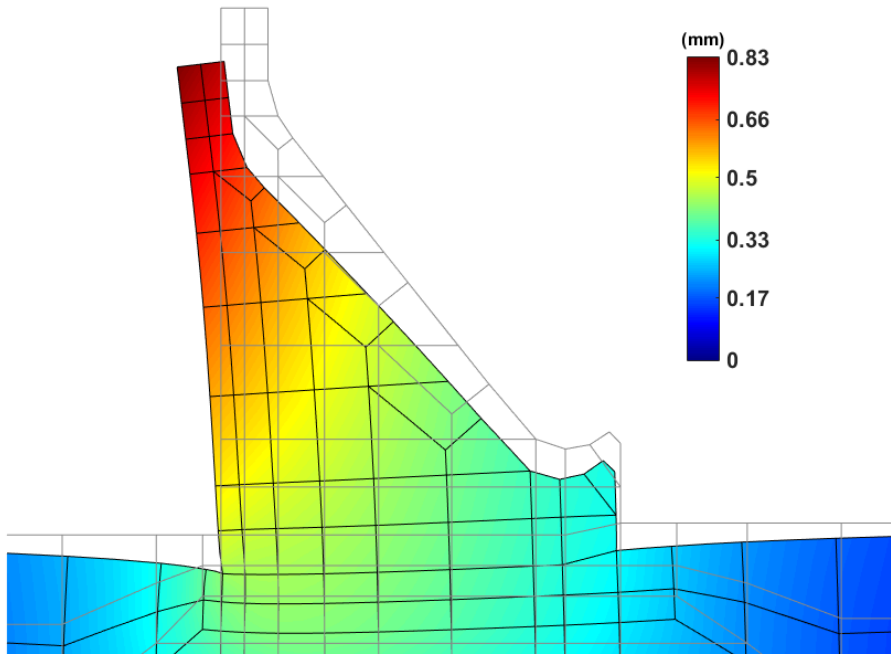
Discretization (EF9N):

NP=871

NE=201

Figure 6.3 – Dam discretization using Lagrangian FE with 9 nodal points (automatically generated with GDams2D1.0)

Deformed Shape / Displacement Field (SW). Color for $|u|$



Principal Stresses (SW)

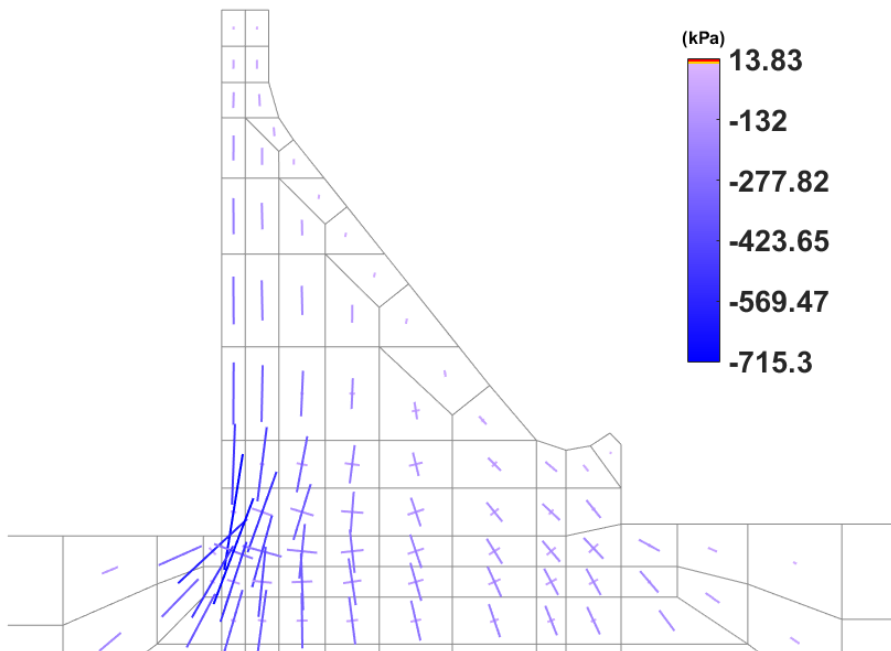
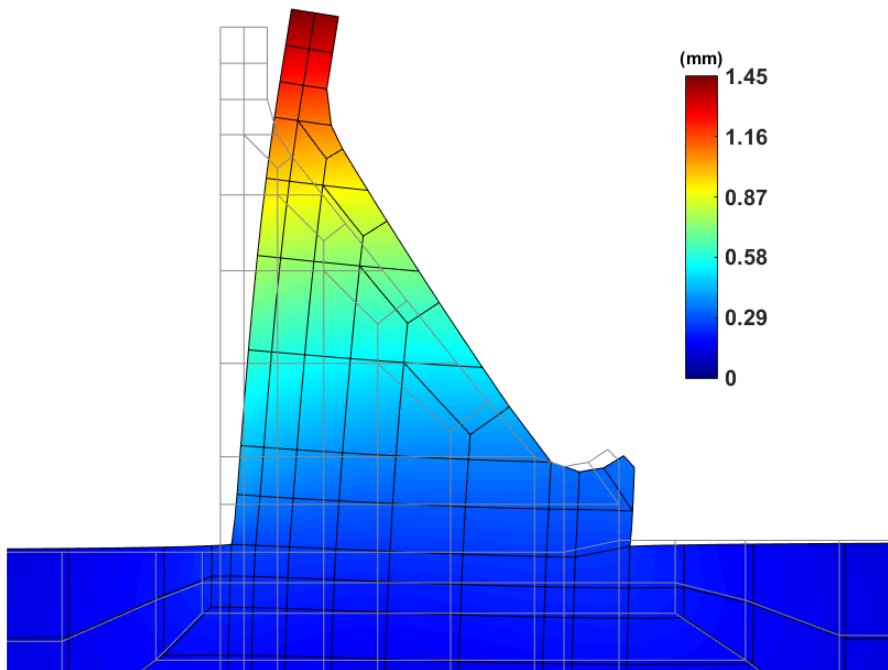


Figure 6.4 – Dam response under self-weight. Displacements and principal stresses (GDams2D1.0)

Deformed Shape / Displacement Field (HP). Color for $|u|$



Principal Stresses (HP)

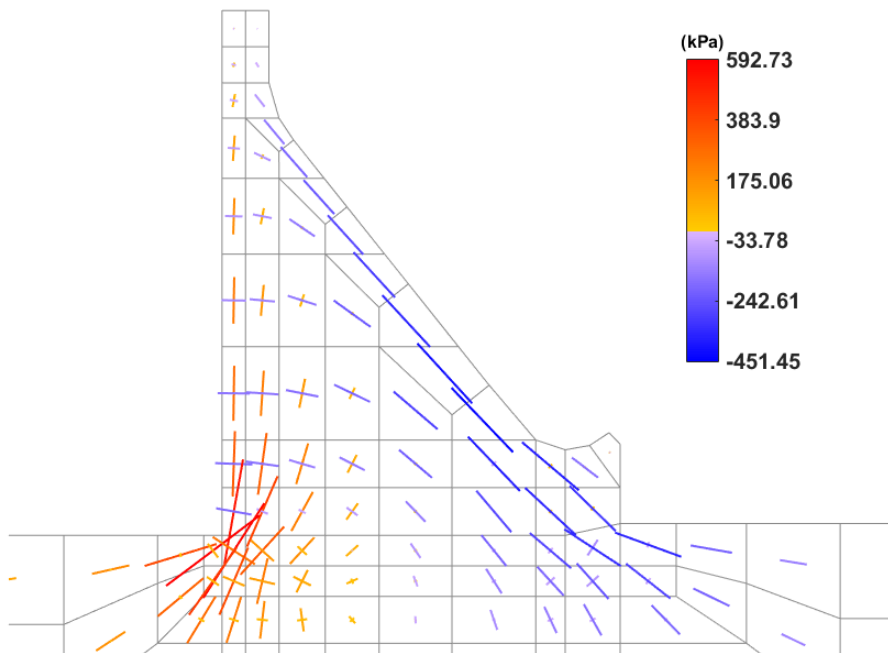
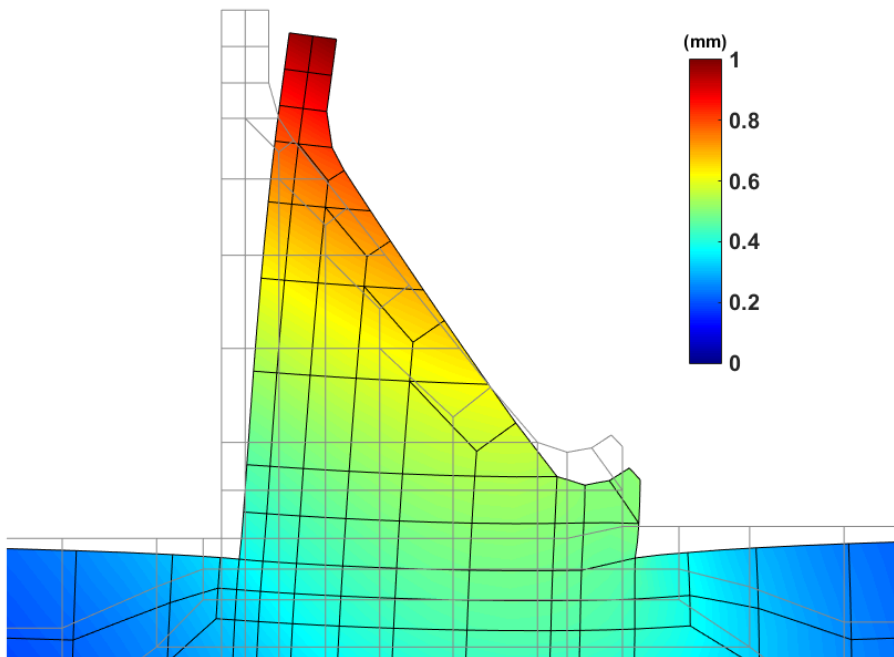


Figure 6.5 – Dam response under hydrostatic pressure. Displacements and principal stresses (GDams2D1.0)

Deformed Shape / Displacement Field (SW + HP). Color for $|u|$



Principal Stresses (SW + HP)

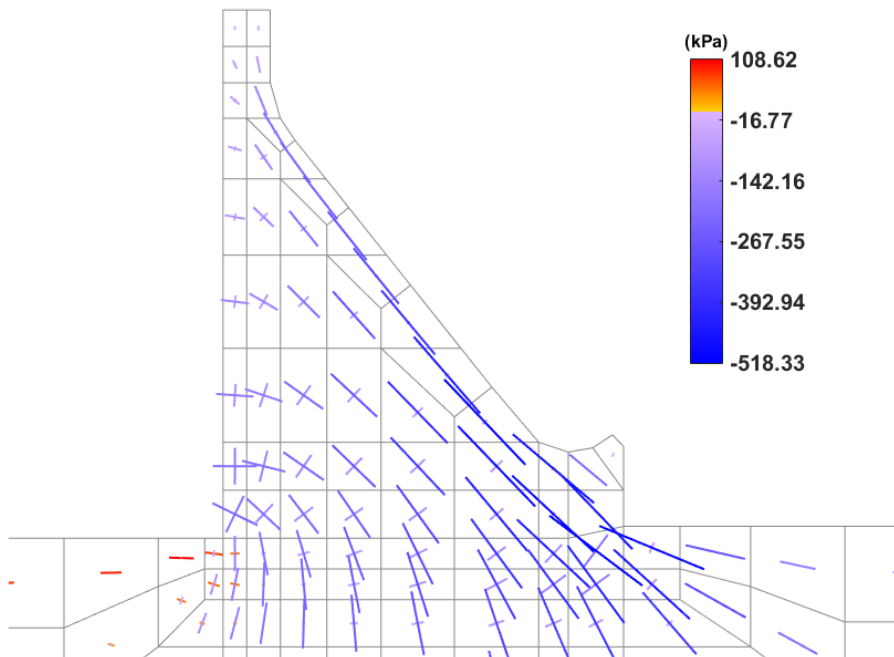


Figure 6.6 – Dam response under self-weight and hydrostatic pressure. Displacements and principal stresses (GDams2D1.0)

The presented dam model can be used for the analysis of the observed dam behavior. In LNEC, The data from dam observation is processed using the program **DamSafe1.0** (Figure 6.7). This program receives the observed data, e.g. displacements histories, and separates the effect of each load, which the structure is subjected.

From the outputs of **DamSafe1.0**, as it is shown in the bottom part of Figure 6.7, the experimental value for the maximum displacement at the crest, due to the hydrostatic pressure, is of about 1.5 mm (full reservoir), accordingly the effects separation. The correspondent displacement computed with the presented FE model (**GDams2D1.0**) is of about 1.4 mm, that is a value perfectly coherent with the identified value (1.5 mm).

Thus, taking into account the good agreement between the dam displacements computed with **GDams2D1.0** and the observed displacements, we can be confident that the program is indeed operational and that the designed model is delivering reliable results, simulating well the actual dam behavior for the main loads, namely for the hydrostatic pressure.

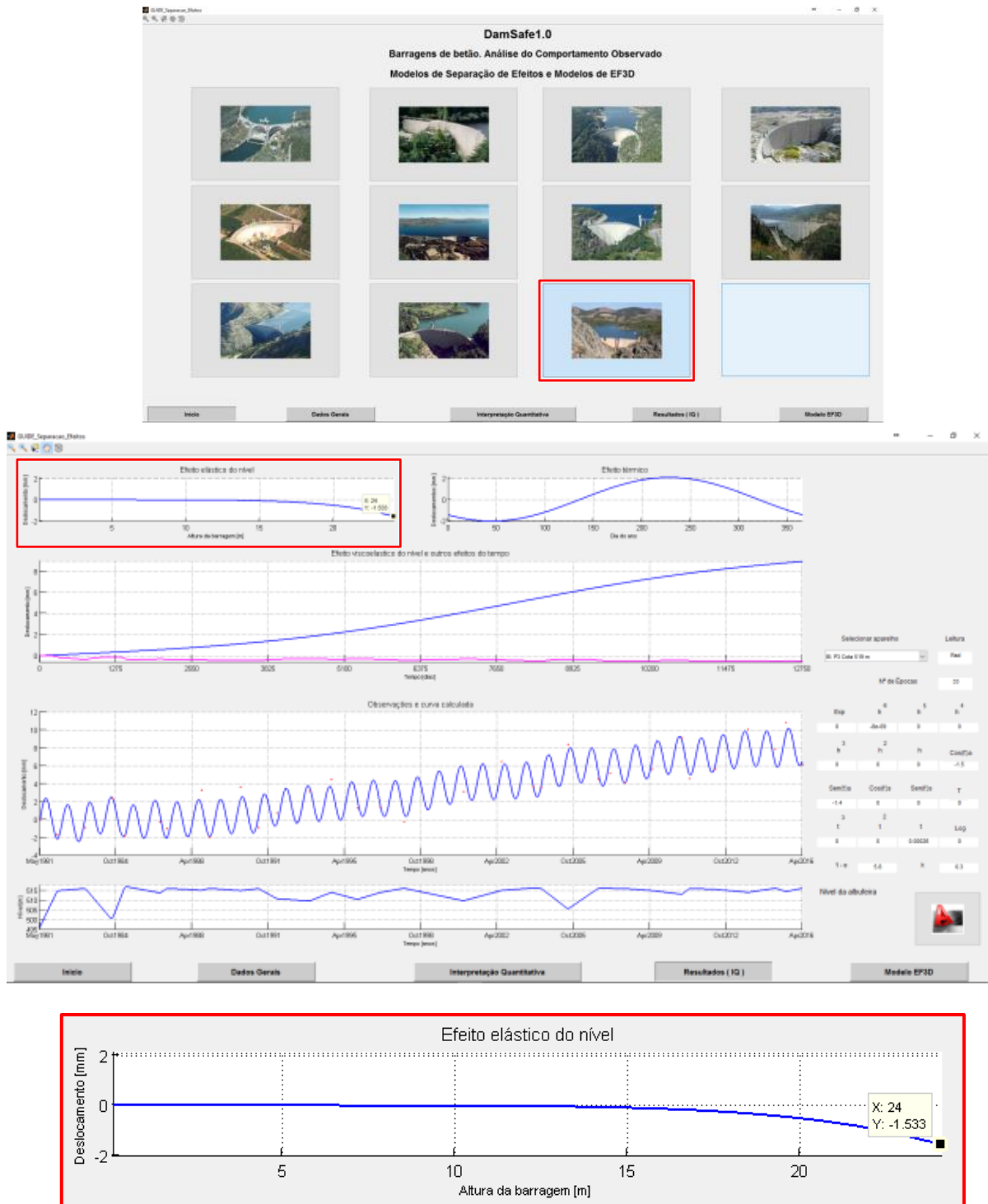


Figure 6.7 – DamSafe1.0. Program for observation data analysis, using effects separation models. Program’s main menu, output window for the studied dam. Zoom on the hydrostatic effect graph

7 | Conclusions

The main objective of this report was the presentation of the FE program, **GDams2D 1.0**, developed for 2D analysis of gravity dams using the finite element method. This initial version of the program is prepared to analyze the structural behavior of gravity dams for static loads, considering linear-elastic behavior, and using quadrilateral Lagrangian finite elements, with 9 nodal points.

The **GDams2D 1.0** program, was developed in MATLAB, and includes a module for automatic generation of meshes with high level of refinement (generated from coarse meshes of quadrilaterals, with 4 nodal points at the vertices). It was designed for easy adaptation to non-linear analyzes, using stress-transfer modules such as those recently developed for the **DamSlide3D** and **DamDamage3D** programs.

After a brief reference to the fundamentals of solid mechanics and to the simplified hypotheses of plane elasticity, the Fundamentals of the Finite Element Method (FEM) were presented, referring in particular the formulation of the four-node, linear and isoparametric, finite element (FE4nodes), with two translation d.o.f per node, and the quadrangular FEs of 9 nodes (FE9nodes) used in **GDams2D 1.0**. Based on some examples of application to simple 2D structures whose response is known analytically, the advantages of FE9nodes was emphasized in relation to FE4nodes and the verification and operability of **GDams2D 1.0** was made using various discretizations.

Finally, the case of a gravity dam (25 m high) was presented. The dam's structural behavior for the main loads, self-weight and hydrostatic pressure, was simulated with **GDams2D 1.0**. The results obtained were analyzed based on the post-processing module of **GDams2D 1.0**, also developed in MATLAB. It was emphasized that this module allows several types of representation of the displacement field and stress field.

Lisbon, LNEC, September 2019

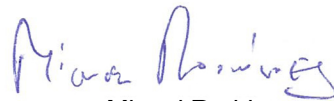
APPROVED

AUTHORS

Head of Modelling and Rock
Mechanics Unit



Luís Nolasco Lamas



Miguel Rodrigues

Doctoral Research Fellow

Head of Concrete Dams Department



António Lopes Batista



Sérgio Oliveira

Assistant Researcher

Bibliographic References

- AdC, 2009 – **Barragem de Penha Garcia. Regras de Exploração.** Águas do Centro, S.A. T568.1.8.
- ARGYRIS, J., 1954 – **Energy theorems and structural analysis**, Aircraft Engineering, 1954 and 1955 (re-printed by Butterworth's Scientific Publications, London, 1960).
- CLOUGH, R.W., 1960 – **The finite element in plane stress analysis**. Proc. 2nd A.S.C.E. Conf. on Electronic Computation, Pittsburgh, Pa., Sept. 1960.
- CLOUGH, R.W., 1965 – **The finite element method in structural mechanics**, in: Stress Analysis, Chapter 7, edited by O.C. ZIENKIEWCZ and G.S. HOLISTER, John Wiley and Sons, Ltd., pp. 85-87, 1965.
- CLOUGH, R.W., 1979 – **The finite element method after twenty-five years: A personal view**, Int. Conf. on Engineering Application of the Finite Element Method, Computas, Veritas Center, Hovik, Norway, p. 1.1, May 1979.
- CLOUGH, R.W., WILSON, E.L. 1962 – **Stress analysis of a gravity dam by the finite element method**, Proc. Symposium on the Use of Computers in Civil Engineering, Laboratório Nacional de Engenharia Civil, Lisbon, Portugal, 1962.
- COURANT, R.L., 1943 – **Numerical Treatment of the Plane Torsion Problem for Multiply-Connected Domains**, in appendix of “Variational Methods for the Solution of Problems of Equilibrium and Vibration”, Bulletin of the American Mathematical Society, vol. 49, pp. 1-23, 1943.
- CNPGB, 1992 – **Large Dams in Portugal.** Comissão Nacional Portuguesa de Grandes Barragens. Retrieved January 3, 2017, from http://cnpgeb.apambiente.pt/gr_barragens/gbportugal/FICHAS/PenhaGarciaficha.htm
- DAES-UCB, 2017 – **Introduction to Finite Element Methods. Part II: Mathematical Formulation of Finite Elements. FEM Convergence Requirements.** University of Colorado at Boulder. Retrieved January 25, 2017, from <http://www.colorado.edu/engineering/cas/courses.d/IFEM.d/IFEM.Ch19.d/IFEM.Ch19.pdf>
- DES-UA, 2008 – **Solid Mechanics Lecture Notes. Engineering Solid Mechanics. Differential Equations of Solid Mechanics. The Equations of Motion.** Department of Engineering Science, University of Auckland. Retrieved January 5, 2017, from http://homepages.engineering.auckland.ac.nz/~pkel015/SolidMechanicsBooks/Part_II/01_DifferentialEquilibriumAndCompatibility/DifferentialEquations_01_Eqns_of_Motion.pdf
- DES-UA, 2008 – **Solid Mechanics Lecture Notes. Engineering Solid Mechanics. Differential Equations of Solid Mechanics. The Strain-Displacement Relation.** Department of Engineering Science, University of Auckland. Retrieved January 4, 2017, from http://homepages.engineering.auckland.ac.nz/~pkel015/SolidMechanicsBooks/Part_II/01_DifferentialEquilibriumAndCompatibility/DifferentialEquations_02_Strain_DisplacementEqns.pdf

- DES-UA, 2015 – **Solid Mechanics Lecture Notes. An Introduction to Solid Mechanics. Linear Elasticity. The Linear Elasticity Model.** Department of Engineering Science, University of Auckland. Retrieved January 4, 2017, from [http://homepages.engineering.auckland.ac.nz/~pkel015/SolidMechanicsBooks/Part_I/Book SM_Part_I/06_LinearElasticity/06_Linear_Elasticity_01_Elastic_Model.pdf](http://homepages.engineering.auckland.ac.nz/~pkel015/SolidMechanicsBooks/Part_I/Book_SM_Part_I/06_LinearElasticity/06_Linear_Elasticity_01_Elastic_Model.pdf)
- FREITAS, J.A.T., 2009 – **Introdução ao Método dos Elementos Finitos: Elasticidade Plana e Tridimensional.** Análise de Estruturas II. Instituto Superior Técnico. Lisbon.
- GHUGAL, Y.; SHARMA, R., 2011 – **A refined shear deformation theory for flexure of thick beams.** Latin American Journal of Solids and Structures. Retrieved January 25, 2017, from <http://www.scielo.br/pdf/lajss/v8n2/a05v8n2.pdf>
- HRENNIKOFF, A., 1941 – **Solution of problems of elasticity by the framework method.** Journal of applied mechanics. 8.4: 169-175
- OLIVEIRA, E. R. A., 1968 – **Theoretical Foundations of the Finite Element Method.** Int. J. Solids Struct., Vol. 4, pp. 929-952. LNEC. Lisbon.
- OLIVEIRA, S., 2000 – **Modelos para análise do comportamento de barragens de betão considerando a fissuração e os efeitos do tempo. Formulações de dano.** Tese de doutoramento. FEUP. LNEC. Lisbon.
- OLIVEIRA, S., 2016 – **Documentação da Unidade Curricular de Modelação de Estruturas com Elementos Finitos.** Curso de Mestrado em Engenharia Civil. Instituto Superior de Engenharia de Lisboa. Lisbon.
- PEDRO, J. O., 1977 – **Dimensionamento de barragens abóbada pelo método dos elementos finitos.** Memória n.º 479. Tese para especialista. LNEC. Lisbon.
- PEREIRA, R., 2011 – **Análise probabilística da segurança ao deslizamento de barragens gravidade de betão.** Dissertação para obtenção do Grau de Mestre em Engenharia Civil - Perfil Estruturas. Faculdade de Ciências e Tecnologia. Universidade Nova de Lisboa. Lisbon.
- SERAFIM, J. L.; CLOUGH, R. W., 1990 – **Arch Dams.** International workshop on arch dams. Coimbra. 5-9 April 1987. A. A. Balkema. Rotterdam. Brookfield.
- TURNER, M. J., CLOUGH, R. W., MARTIN H. C. and TOPP, L. J., 1956 – **Stiffness and Deflection Analysis of Complex Structures** . Journal of the Aeronautical Sciences, Vol. 23 No. 9, 1956 pp. 805-823.
- ZIENKIEWICZ, O.C., and CHEUNG, Y.K, 1967 – **The Finite Element Method in Structural and Continuum Mechanics**, McGraw-Hill publishing Coy Ltd, London, p148.
- ZIENKIEWICZ, O.C., 1971 – **The Finite Element Method in Engineering Science**, 2nd ed. McGraw-Hill, New York, 1971.
- ZIENKIEWICZ, O. C.; TAYLOR, R. L.; ZHU, J. Z., 2005 – **The Finite Element Method: Its Basis and Fundamentals.** 6th Edition. Elsevier Butterworth-Heinemann. Burlington, England.

